Preparation and photoelectrical properties of C60-PEG/conducting polymer composite material

（C60-PEG / 導電性高分子複合材料の作製と光電特性）

Huiqiu Zhang

Doctoral Program in Advanced Materials Science and Technology

Graduate School of Science and Technology

Niigata University

2015

Content

Chapter 1

General Introduction

1.1 Fullerene and derivatives

Fullerenes possess interesting electrochemical, [1,2] photophysical,[3] optical,[4] semiconducting,[5] superconducting,[6–8] magnetic [9–11] and aggregation[12] properties. Based on the functionalization and study of new fullerene derivatives, a new research field has emerged in recent years, those derivatives intends to employ the properties of these carbon hollow clusters in different fields.

Table 1-1 Solubility of C60 fullerene in various solvents

Solvents	Solubility (mg/mL)
Water	0
Methanol	0
THF	0
Acetone	0.001
n-Hexane	0.043
Chloroform	0.16
Benzene	1.7
Toluene	2.8
o-Dichlorobenzene	27

Because of the availability, high symmetry and low price, C60 is the most studied and widely used of the fullerenes. Upon functionalization, the solubility of C60 in organic solvents is increased, enhancing its proccessability. Some of the most promising fields of application of these materials, include non-linear optics, artificial photosynthesis and the preparation of photoactive well-organized films and nanostructures. Because they can be used as artificial models of the photosynthetic reaction center to transform light into chemical energy, the research on donor–

acceptor systems involving fullerenes has attracted a lot of attention. In the natural photosynthetic reaction center, [13] several photoactive units are coupled together, so that several photoinduced electron transfer (PET) events take place after irradiation, giving a long distance and long-lived charge separated state in which the energy is stored. The easiest approach to an artificial model consists of two different units, an electron-donor and an electron-acceptor linked together. Fullerenes and especially C60 have been widely used electron-acceptors, since they have a high electron affinity[1,14,15] and small reorganization energy.[16] The electrons are highly delocalized in the three-dimensional p-system.[17] Therefore fullerenes have shown to give very stable radical pairs.[3]

1.2 Conducting polymer

Polymers have been used as insulating materials for long time. For example, metal cables are coated in plastic to insulate them. However, there are at least four major classes of semiconducting polymers that have been developed so far. They include conjugated conducting polymers, charge transfer polymers, ionically conducting polymers and conductively filled polymers.

Conducting polymers have been a hot research area for many academic institutions since their discovery in the mid-1970s, such as polypyrrole, polythiophene, polyaniline, and sulfonated polyaniline. They are all complex, dynamic structures that captivate the imagination of those of us involved in intelligent material research.[18-22] which has supported the industrial development of conducting polymer products and has provided the fundamental understanding of the chemistry, physics, and materials science of these materials. In particular, the Royal Swedish Academy of Sciences has decided to award the Nobel Prize in Chemistry for 2000 to three scientists who have revolutionised the development of electrically conductive polymers: Alan MacDiarmid, Alan Heeger, and Hideki Shirakawa.

Figure 1-1 The three discoverers of the first conducting polymer: Alan Heeger, Alan MacDiarmid, and Hideki Shirakawa.

Conducting polymers consist of polymers which have unique conjugated backbone structures that facilitate the delocalization of electrons along those chains. The potential applications of conducting polymers have been discussed at length in numerous reviews.[23-29] such as transistors, light-emitting diodes, solar cells, etc. Polymers have the potential advantages of low cost and that they can be processed, such as film.

The conjugated structure with alternating single and double bonds or conjugated segments coupled with atoms providing p-orbitals for a continuous orbital overlap seems to be necessary for polymers to become intrinsically conducting. This is because just as metals have high conductivity due to the free movement of electrons through their structures, in order for polymers to be electronically conductive they must possess not only charge carriers but also an orbital system that allows the charge carriers to move. The conjugated structure can meet the second requirement through a continuous overlapping of π-orbitals along the polymer backbone.

Poly(3,4-ethylenedioxythiophene), abbreviated PEDOT, is regarded as

one of the highlights, placed at the end of this short history. The huge number of scientific PEDOT publications and patents, the large quantities of PEDOT-derived products commercially sold every year and the remarkable impact of PEDOT on daily-life goods show the importance of PEDOT. PEDOT:PSS, or poly(3,4-ethylenedioxythiophene) poly (styrenesulfonate), was already mentioned as a prominent example in the Advanced Information of the Nobel Committee for Chemistry and the Royal Swedish Academy of Sciences regarding the year 2000 prize.

Table 1-2 Selected Physical Properties of EDOT

	Physical Properties
Viscosity (20°C)	11 mPa·s
Density (20°C)	1.34 g/cm^3
Melting point	10.5°C
Boiling point (1013 mbar)	225°C
Vapor pressure (20°C)	0.05 mbar
Vapor pressure (90°C)	10 mbar
Solubility in water (20°C)	2.1 g/l
Flash point	104°C
Ignition temperature	360°C

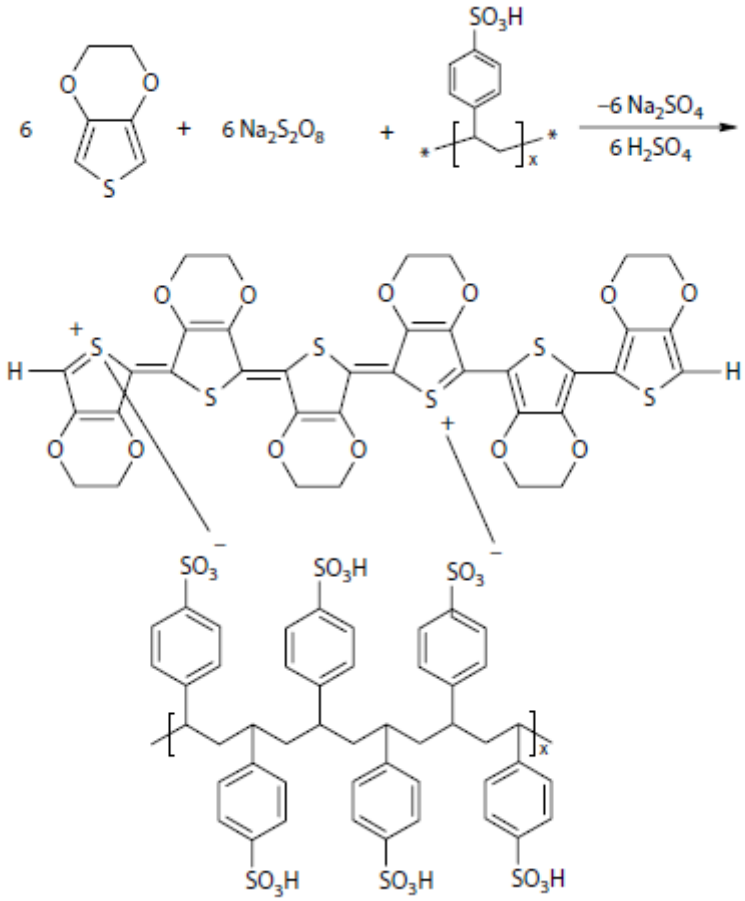

Figure 1-2 EDOT oxidation to PEDOT:PSS.

1.3 Organic semiconductors

Organic semiconductors include small molecules, oligomers (short polymers) and polymers. There are several reasons to use organic materials for photovoltaic solar cell applications. Most important is the peculiar advantages of organic materials:

- they can be processed easily using spin coating or doctor blade techniques (wet-possessing) or evaporation through a mask (dry-processing);
- amounts of organic materials are relatively small (100 nm thick films) and large scale production(chemistry) is easier than for inorganic materials (growth processes);
- they can be tuned chemically in order to adjust separately band gap,

valance and conduction energies, charge transport, as well as solubility and several other structural properties;

- the vast variety of possible chemical structures and functionalities of organic materials (polymers, oligomers, small molecules) favour an active research for alternative competitive materials with the desired PV properties. Original materials and structures can also be covered by patents.

Polymers, oligomers, small molecules, all organic semiconductors share in common part of their electronic structure. It is based on conjugated π electrons. By definition, a conjugated system is made of an alternation between single and double bonds. Ethene, butadiene and benzene are basic representative elements of conjugated systems [30]. The essential property which comes out from conjugation is that the π electrons are much more mobile than the σ electrons; they can jump from site to site between carbon atoms with a low potential energy barrier as compared to the ionisation potential. The π electron system has all the essential electronic features of organic materials: light absorption and emission, charge generation and transport. Each carbon atom in a conjugated system has 3 nearest neighbours with which it forms 3 equivalent σ bonds made from the trigonal sp^2 hybridisation of 3 valence atomic orbitals of the carbon atom: 2s, 2px and 2py for instance [31]. For such a hybridisation state, the fourth orbital 2pz lies perpendicular to the σ bond plane. It is the lateral overlap of these out of plane 2pz atomic orbitals which gives the πbonds. In most molecules , double bonds are localised and the two extreme positions are usually not equivalent. A more general definition of a conjugated system would be an ensemble of atoms whose p-orbitals overlap.

Transport and mobility in organic materials require a knowledge of the charged species. A review of transport properties is given by Schott [32]. Energy levels of the charges are usually determined by cyclic voltametry for materials in solution. They can be characterized by XPS or UPS (X-ray

and UV photoelectron spectroscopies) for solid materials. In small molecules, charged species are localized spatially, they are simply the cation (positive) and anion (negative) radicals. In polymers, the electron–phonon coupling leads to the so-called polarons which are charges dressed by a reorganization of the lattice [33]. Polarons may be regarded as defects in conjugated polymer chains. Such defect stabilises the charge which is thus self-trapped as a consequence of lattice deformation. So in the vast majority of organic semiconductors, transport bears all characteristics of a hopping process in which the charge (cation or anion) propagates via side to side oxidation–reduction reactions. One must distinguish between intramolecular charge transport along a conjugated polymer chain and intermolecular charge transport between adjacent molecules or polymer chains.

1.4 Polymer solar cells

Polymer solar cells are a type of organic solar cell with active layer composed of polymer and/or other organic semiconductors. The simplest type of polymer solar cells contains a substrate (rigid substrate such as glass or flexible substrate such as plastic), an anode (an electrode for collecting holes), an active layer and a cathode (another electrode for collecting electrons). While light is absorbed by the active layer, the electrons and holes generated are then extracted by the cathode and anode respectively. In most of polymer solar cells, a hole-transporting layer (HTL, in between anode and active layer) or an electron-transporting layer (ETL, in between cathode and active layer) usually exists for enhancing device performance. Figure 1-3 (a) shows the schematic diagram of a typical polymer solar cell with active layer composed of poly(3-hexylthiophene) (P3HT) and [6,6]-phenyl-C61-butyric acid methyl ester (PCBM). In this structure, tin doped indium oxide (ITO) is the anode while aluminum (Al) is the cathode, poly (3,4-ethylenedioxythiophene): poly(styrenesulfonate) (PEDOT:PSS) layer is the HTL used for enhancing hole transport between

the active layer and ITO. This structure of polymer solar cells is called the conventional structure and is most widely applied and investigated due to its simple fabrication method. Besides conventional structure in which the bottom electrode (electrode close to the substrate) is an anode, there is inverted structure in which the bottom electrode is a cathode (Figure 1-3 b).

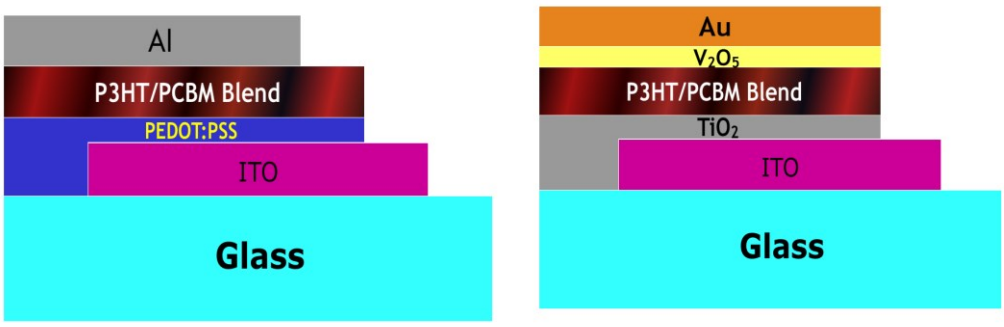

(a) (b)

Figure 1-3 (a) the conventional structure and (b) the inverted structure of polymer solar cell

The active layer of polymer solar cells usually contains two kinds of organic semiconductors, e.g. polymers and fullerene derivatives, operating as electron donors and electron acceptors (or called donor and acceptor for short) respectively. The process of converting light into electricity in a polymer solar cell can be described as follows (Figure 1-4):

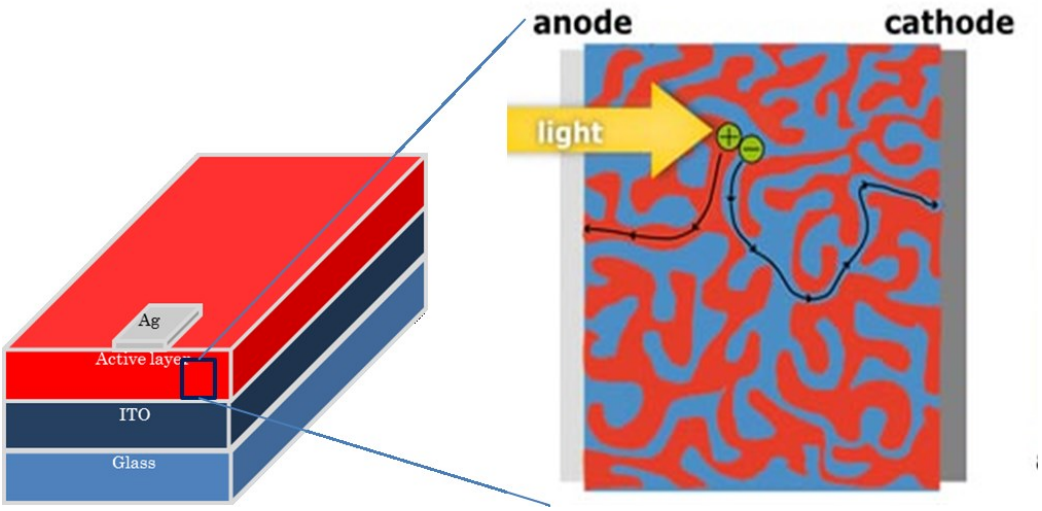

Figure 1-4 physical process of converting light into electricity in a bulk heterojunction solar cell.

The fundamental process of photo energy conversion in a polymer solar cell can be divided into four steps: 1) light absorption and exciton generation, 2) exciton diffusion, 3) exciton dissociation, 4) charge transportation and charge collection [34]. The first three steps can be represented using the expressions below [34,35]:

$$D + A \overset{h\nu}{\rightleftharpoons} D^* + A$$
$$D^* + A \rightleftharpoons [D^*, A]$$
$$[D^*, A] \rightleftharpoons [D^{+\bullet}, A^{-\bullet}]$$
$$[D^{+\bullet}, A^{-\bullet}] \rightleftharpoons D^{+\bullet} + A^{-\bullet}$$

Where D, A represent a donor and an acceptor molecule, respectively.

In a polymer solar cell, light absorption usually occurs in polymer (i.e. donor) region due to its low band gap which allows its absorption spectrum to have a higher overlap with solar spectrum. A photon absorbed by the active layer leads to an electron-hole pair bound by Coulomb force (exciton). The photoexcited donor exciton usually has binding energy in the order of hundred mill-electronvolts (meV) which is a lot higher than exciton binding energy in inorganic materials, which is typically of the

order of tens of meV or several meV [36]. Thus certain amount of energy is required for separating exciton into free carriers. Charge transfer happens when this donor exciton diffuses to the interface of donor/acceptor materials. An electron can be transferred from donor exciton to the acceptor at the donor/acceptor interface due to the driving force induced by the energy difference between the lowest unoccupied molecular orbitals (LUMOs) of the donor and acceptor [34]. This results in a Coulombically bound electron and hole pair located in spatially separate regions across the donor/acceptor interface and is called charge chargetransfer exciton (CT exciton) [37]. Detailed mechanism behind the dissociation of CT excitons is still unclear, however it is generally believed that the abrupt change of potential at the interface causes the generation of free carriers [38]. This free electron and hole then transport to the corresponding electrodes and extracted by the contacts.

To characterize a polymer solar cell, current-voltage (I-V) measurement is usually applied and an I-V curve (Figure 1-5) is obtained.

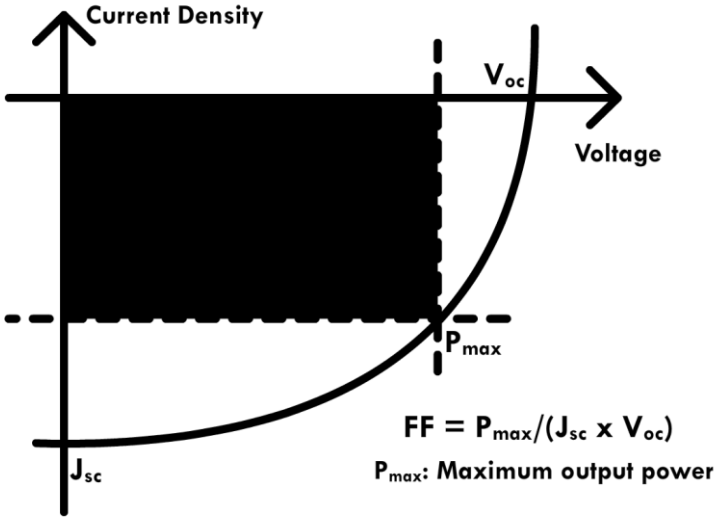

Figure 1-5 Schematic I-V curve of polymer solar cell under illumination

The performance of a polymer solar cell is described by its short circuit current density (Jsc), open circuit voltage (Voc), fill factor (FF) and power

conversion efficiency (PCE) following the equation below:

$$PCE = \frac{J_{sc} \times V_{oc} \times FF}{P_{in}},$$

Pin is the input power density of light.

In polymer solar cells, V_{oc} is found to be dependent on the difference between the highest occupied molecular orbital (HOMO) level of the donor and the lowest unoccupied molecular orbital (LUMO) level of the acceptor [36]. Scharber et al. [39] studied 26 different polymer/PCBM based solar cells and found almost linear dependence between the HOMO of donor and Voc. On the other hand, J_{sc} is determined by light absorption, exciton dissociation, charge transport and charge collection. Band gaps of semiconducting polymers are usually higher than 1.9 eV [36, 39], thus wavelength over 650 nm can not be absorbed. Semiconducting polymers with lower band gaps are essentially needed for efficiency enhancement. Researches in finding low band gap polymers have been very popular in the last decade and tremendous results have been achieved [40-44]. Moreover, to achieve both large V_{oc} and broad absorption band, conjugated polymers with deeper HOMO level and small band gap are required [42-44]. For the exciton dissociation in polymer solar cells, due to the low mobility and limited life time of excitons, the diffusion lengths of excitons are usually less than 10 nm. Thus as discussed before, polymer and fullerene derivative with phase separation of only several nanometers is required for efficient exciton dissociation at the interface. After exciton dissociation, free holes and electrons must be transported via interpenetrated pathways of polymer and fullerene derivative towards the electrodes to produce the photocurrent which relates to the charge carrier mobility. In general, charge carrier mobility in polymer solar cell is lower than that in the inorganic counterpart. Hole mobility in the polymer and electron mobility in the

fullerene derivative are usually not balanced[36]. Different material combinations and methods have been tried and polymers and fullerene derivatives with improved charge carrier mobility have been synthesized [36, 41]. It is also found that electron and hole mobility can be tailored by changing the weight ratio of polymer and fullerene derivative in the blend and further enhanced by post annealing [36, 45]. Efficient charge collection at the electrodes requires energy level alignment between the organic semiconductors and the electrodes. The work function of ITO is relatively large (~4-5 eV) which makes it suitable for hole collection. However, HOMO of polymer is usually more than 5 eV below the vacuum level [46]. Thus, a thin layer of organic semiconductor with large HOMO level (such as PEDOT:PSS) or metal oxide with high work function can be used to lower the energy barrier and improve the charge collection atthe anode. Besides, PEDOT:PSS is also found to smooth the surface of ITO andreduce the possibility of short circuits [40]. Organic solar cells can be generally categorized into single layer organic solar cells, bilayer organic solar cells (also called two layer organic solar cells or planar heterojunction solar cells) and bulk heterojunction solar cells (Figure 1-6) by their respective structures. In general, the development of organic solar cells is from the simplest single layer organic solar cells to bilayer organic solar cells and then to the more recent bulk heterojunction organic solar cells.

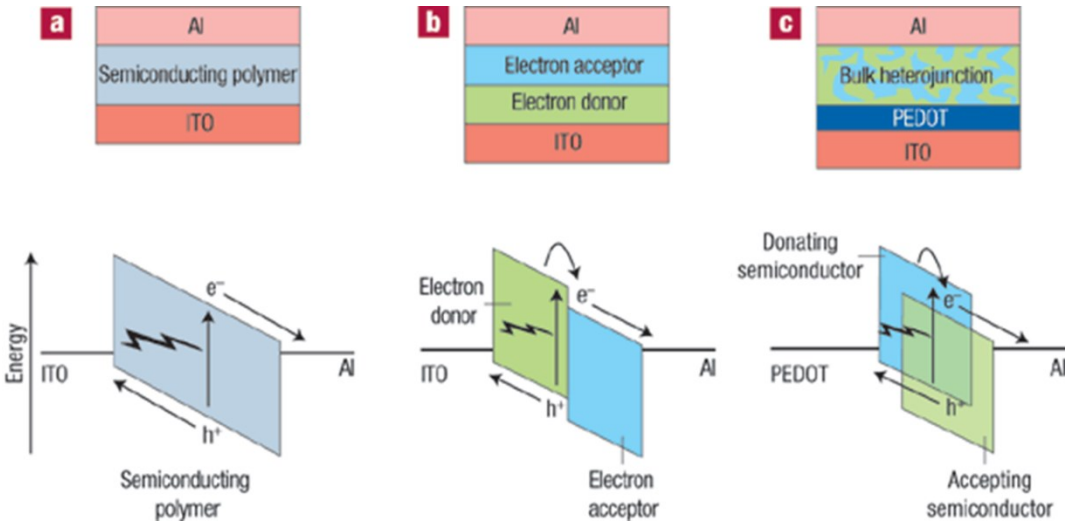

Figure 1-6 Three different forms of device architecture (a) single-layer device(b) two-layers device(c) bulk heterojunction device

A single layer organic solar cell is of sandwiched structure with an organic layer covered by a low work function metal and a high work function metal (or ITO) [47]. In this case, exciton dissociation occurs only at the organic-metal interface. Due to the limited exciton diffusion length and organic-electrode contact area, power conversion efficiencies of such cells are usually quite low (below 1%) [47]. Thus, a more complicated structure is required for efficiency enhancement. The idea of two-layers organic solar cells became popular when Tang reported a two-layer organic photovoltaic cell with efficiency around 1% in 1980s [48]. In his device, ITO coated glass was used as the substrate, several hundred angstrom of copper phthalocyanine (CuPc) and perylene tetracarboxylic derivative (PTCD) was deposited in sequence by vacuum evaporation as the active layer, finally a silver (Ag) layer was deposited on top of PTCD as the cathode. In bilayer structure, exciton separation happens not only at organic/metal interface, but also at donor/acceptor interface. Intensive investigations on bilayer organic solar cells were carried in 1980s and 1990s, but not much improvement of PCE was found over Tang's 1% solar cell [49]. On the other hand, systematical studies of bilayer organic solar cells showed that

performance of such devices strongly depended on donor and acceptor layer thickness [50]. In 1999, Pettersson et al. [51] modeled on poly(3-(4'-(1",4",7"-trioxaoctyl)phenyl)thiophene) (PEOPT) / fullerene (C60) bilayer solar cell and discovered that exciton diffusion length in PEOPT and C60 were only 4.7nm and 7.7 nm respectively. High efficiency polymer solar cells require a good combination of efficient light absorption and charge carrier transport. This certainly can not be achieved by bilayer structure due to the limited exciton diffusion length (if active layer is thin, light absorption is not complete; if layer is thick, charge dissociation is not efficient). Based on this result, bilayer solar cells with donor and acceptor thickness each around 10~20 nm would be good for efficient exciton dissociation, but this is too thin for efficient light absorption (typical thickness for efficient light absorption is more than 100 nm). Thus bilayer structure was found to be not suitable for high efficiency polymer solar cells. To solve the above problem, bulk heterojunction structure provides an excellent solution. In a bulk heterojunction solar cell, donor and acceptor materials are deposited together resulting in an intermixed structure. In this way, a polymer solar cell with small sub-domains (donor/acceptor mixture locally) can be achieved with less constraint on the total active layer thickness. In 1991, Hiramoto et al. [52] fabricated organic solar cells with active layer comprised of perylene tetracarboxylic derivative (Me-PTC) and metal-free phthalocyanine (H2PC) which showed 0.7% efficiency under white light intensity of 100 mW/cm^2. It was found that insertion of a mixed interlayer in between the original bilayer structure could result in a J_{sc} enhancement over two-fold. In the research of bulk heterojunction solar cells, different donor/acceptor material combinations have been tried, among which P3HT/PCBM system is found to be promising [40, 53-55.] In 2005, two groups reported on P3HT/PCBM based bulk heterojunction solar cells with efficiency approaching 5% [54, 55]. In their papers, annealing devices at elevated temperature was found to improve the

J_{sc} and FF dramatically. Ma et al. [54] used X-ray diffraction (XRD), transmission electron microscopy (TEM) and atomic force microscopy (AFM) to examine the active layer before and after annealing. It was argued that enhancement in the device performance by annealing was due to improved morphology and crystallinity of the active layer. The improved phase separation between P3HT and PCBM induced better exciton dissociation at the interface and the highly crystallized P3HT increased its hole mobility. Driven by these exciting results, extensive investigations on bulk heterojunction solar cells (especially on P3HT/PCBM system) were carried out by more and more researchers. Several fabrication parameters including donor/acceptor weight ratio, layer thickness, annealing time and temperature etc. were all found to be influential on the solar cell performance. Besides annealing, several other techniques were also tried for efficiency enhancement including solvent annealing [56, 57], nanoimprinting [58, 59], insertion of buffer layer [60, 61], incorporation of light trapping structure [62] etc. Meanwhile, systematical studies and theoretical calculation of P3HT/PCBM based bulk heterojunction solar cells were also carried out to understand the physics behind [45, 63]. These studies are not only helpful in understanding P3HT/PCBM system but also useful in the research of other donor/acceptor systems. Although P3HT/PCBM system showed promising performance, efficiency of solar cells based on this system was still not good enough for commercialization. Certain drawbacks of P3HT/PCBM system include the relatively large band gap of P3HT (low solar spectrum coverage) and the small difference between HOMO of P3HT and LUMO of PCBM (low Voc). In recent years, bulk heterojunction solar cells with efficiency over 6% have been achieved by the use of some low band gap polymers and fullerene derivatives [42-44, 64]. Besides aiming for high efficiency organic solar cells, large scale production and applications of organic solar cells were also studied. In particular, metal grid was used to enhance the conductivity of ITO

electrode for large area solar cells [65, 66], semi-transparent and flexible organic solar cells were also made utilizing their advantages for future commercialization [67, 68]. It is generally accepted that bilayer solar cells exhibit much lower efficiency than bulk heterojunction solar cells, but one thing worth noticing was a recent report of all-solution-processed P3HT/PCBM bilayer solar cells done by Ayzner et al. [69]. In that paper, P3HT and PCBM were dissolved in o-dichlorobenzene (ODCB) and dichloromethane (DCM) separately and spin-cast in sequence on top of PEDOT:PSS coated conductive glass. DCM was chosen as it only slightly dissolved P3HT and PCBM was sufficiently soluble in DCM. Several devices with annealing before top electrode deposition showed efficiencies around 3.5% which was quite close to that of bulk heterojunction structure. It was claimed that spin-coated PCBM layer did not intermix with the underlying P3HT layer or affect its morphology during the fabrication (spin-coating and annealing). Thus a clear boundary was presented in between P3HT and PCBM layer ensuring its nature of bilayer. This interesting finding had drawn attention of several other groups. Lee et al. [70] and Moon et al. [71] challenged the validity of bilayer structure and believed that P3HT/PCBM bilayer solar cells produced by Ayzner et al. had intermixed active layer. Lee et al. analyzed the distributions of P3HT and PCBM throughout the active layer using Xray photoelectron spectroscopy (XPS) and argued that interdiffusion of P3HT and PCBM had happened even before thermal annealing. Moon et al. examined the cross-section morphology of both layer-by-layer and bulk heterojunction P3HT/PCBM using TEM and found no significant difference between the two.

There has been a great improvement in the polymer photovoltaic cell efficiencies of bulk heterojunctions fabricated by polymer:fullerene blend films in the past decade. In order to improve efficiency, novel materials with lower energy gaps need to be developed to improve the coverage of the solar spectrum.

1.5 Biomimetic

The interface between biology and materials science has rapidly emerged to be at the forefront of materials research. Nevertheless, the study of biological systems as structures dates back to the early parts of the twentieth century. The nascent field of biological-based materials science can be divided into three broad (and overlapping) areas:

I. Biological materials – the study of natural materials (e.g. bone, feathers, skin).
II. Biomimetics or bioinspired materials design – synthesis of novel materials, devices, and structures inspired on biology.
III. Biomaterials – the application of materials in the biomedical arena (e.g. implants).

Bio-inspired design is a cutting edge field of inquiry and practice, founded by thinkers such as Steele (bionics, 1950s), Schmitt (biomimetics, 1950s), and French (biologically inspired design, 1988) [72]. Many successful products have resulted from this approach or way of designing, drawing on form, function, and process-based inspiration from biology [73] and dating back to the 19th century, including barbed wire, Tiffany lamps, the Wright glider, the design of Central Park in Manhattan [74], and many more.

The design of materials involves consideration of a wide number of structural elements which, on their turn, determine the resulting properties. The most important structural components are [75]:

- Atomic/molecular design.
- Nanostructures and boundaries.
- Dislocation and other defect structures.
- Cells and other substructures (size, morphology, structure, orientation).
- Grain size, orientation, morphology and structure.
- Particle and precipitate coherence, shape and distribution.
- Orientation distributions.
- Phase relationships and morphologies.

- Design of interfaces at all length scales.
- Phase transformations.

Materials design is a mature and highly developed field with massive investments globally. The approaches used range from fundamental thermodynamics and density-funtional theory to Edisonian trial-and-error developments. Evolutionary and revolutionary changes have pushed the performance of synthetic materials (alloys, polymers, ceramics, and composites) to their limits. Hence, novel design concepts have to be implemented if we are to make progress. What seems to be effortless in a biological system that produces complex, multifunctional materials can, indeed, be translated to processing of synthetic materials. Layered structures, such as abalone nacre, exhibit high toughness values despite low fracture toughness constituents. For example, it has been shown that for metal/metal, polymer/polymer and glass/polymer laminates, thinner layers produce a tougher composite than do thicker layers [77,79–81]. This suggests that the scale and hierarchy are important considerations in materials design.

Challenges and opportunities for bioinspired materials development include [75-78,82,83]:

- Synthetic constituents to produce hierarchical materials with useful performance over a broad range of environmental conditions (e.g. temperature, pressure, humidity).
- Wear-resistant materials with low friction coefficients for joints and bearings (e.g. knee joints).
- Synthetic adhesives that recreate the sturdiness and toughness of biological adhesives (e.g. gecko feet).
- Composites with high volume fractions of the reinforcement (e.g. nacre).
- Multifunctional materials.
- Electro-optical devices.

- Manufacturing and synthesis techniques under ambient conditions.
- Self-assembled materials.
- Self-healing, environment-adaptable materials.

Additionally, a systems approach must be taken to put theory into practice. Biological systems adapt to changing ambient conditions, continually refining and adjusting shape, chemical and mechanical signaling. Some of the challenges include [75]:

- Strong, durable interfaces between the hard and soft constituents.
- Tribological joints with low friction coefficients and remarkable durability.
- Mechanistic understanding and analysis methods for deformation and failure of complex systems.
- Energy-absorbing mechanisms of rigid biological composites.
- Platelet and surrounded plate analytical concepts; and
- Moisture friendly synthetic systems.

It is clear that the design of materials and structures inspired in nature involves special challenges not encountered earlier. Traditional design has followed disciplinary lines, but bioinspired design will require multidisciplinary teams of engineers (design and structure) and life scientists (biochemistry, biology, physiology, anatomy molecular biology) to develop materials with complex, hierarchical structures.

1.6 Objectives of this work

To fabricate and measure photoelectrical properties of polymer solar cell devices by using C60-PEG/PEDOT material and improving the Power conversion efficiency (PCE), the following research has been carried out: Preparation of C60- PEG/PEDOT composite material by using chemical oxidative polymerization under low temperature organic-solvents processed. Then fabrication of photovoltaic devices of polymer solar cells by using C60- PEG/PEDOT composite material and measurement their

photoelectric properties. To improve the PCE, many methods had been implemented, in which biomimetic and other simple method were effective, including mimicking moth eye microstructure film and changing molar ratio of C60 and PEG. Preparation of microrods Structure C60- PEG /PEDOT Composite Film by Template method and application for Organic Photovoltaic Devices

In Chapter 2, C60-PEG/PEDOT gel by chemical oxidative polymerization under low-temperature organic-solvents processed has been prepared. PEDOT was synthesized inside of C60-PEG gel, and that the C60-PEG/PEDOT gel has an amorphous structure on contrary to C60-PEG crystalline structures. Then the polymer solar cells device using this composite material has been fabricated, and UV response of C60-PEG/PEDOT device was much higher than C60-PEG device. PCE of C60-PEG/PEDOT device was about 1.2×10^{-3}%. It was expected that all organic solvent polymer solar cells with new interpenetrate network structure using C60 derivate and conductive polymer composite materials will be utilized when PCE would be improved in the future.

In Chapter 3, Mimicking the unique antireflection functionalities of moth eye microstructure, microrods structure film with many of nanoscale layered sheets around the rod were fabricated by template method at room temperature. UV-Vis absorption spectra shown a significantly red shift of microrods structure film from flat structure film, it was estimated that it would be attributed to bandgap narrowing along with the structure changing. Then CV measurement provided a reference that bandgap of microrods structure film was 0.08eV narrow than the flat structure film. The result of PCE was more higher than the flat structure one, in which the J_{sc} had a remarkable increase revealed that the microrods structure not only was able to trap more light to improve the photoinduced chage carrier density, but can improve the mobility of charge carriers.

Conclusions are presented in Chapter 5.

References

1. L. Echegoyen and L.E. Echegoyen, Acc. Chem. Res., 1998, 31, 593–601.
2. C. Bruno, I. Doubitski, M. Marcaccio, F. Paolucci, D. Paolucci and A. Zaopo, J. Am. Chem. Soc., 2003, 125, 15738.
3. D.M. Guldi and M. Prato, Acc. Chem. Res., 2000, 33, 695–703.
4. L.W. Tutt and A. Kost, Nature, 1992, 356, 225.
5. R.C. Haddon, A.S. Perel, R.C. Morris, T.T.M. Palstra, A.F. Hebard and R.M. Fleming, Appl. Phys. Lett., 1995, 67, 121.
6. E. Dagotto, Science, 2001, 293, 2410.
7. P. Grant, Nature, 2001, 413, 264.
8.A.F. Hebard, M.J. Rosseinsky, R.C. Haddon, D.W. Murphy, S.H. Glarum, T.T.M. Palstra, A.P. Ramirez and A.R. Kortan, Nature, 1991, 350, 600.
9. P.M. Allemand, K.C. Khemani, A. Koch, F. Wudl, K. Holczer, G. Gruner and J.D. Thompson, Science, 1991, 253, 301.
10. A. Lappas, K. Prassides, K. Vavekis, D. Arcon, R. Blinc, P. Cevc, A. Amato, R. Feyerherm, F.N. Gygax and A. Schenk, Science, 1995, 267, 1799.
11. B. Narymbetov, A. Omerzu, V.V. Kabanov, M. Tokumoto, H. Kobayashi and D. Mihailovic, Nature, 2000, 407, 883.
12. D.M. Guldi, F. Zerbetto, V. Georgakilas and M. Prato, Acc. Chem. Res., 2005, 38, 38.
13. The Photosynthetic Reaction Center, Academic Press, San Diego, 1993.
14. F. Arias, L. Echegoyen, S.R. Wilson and Q. Lu, J. Am. Chem. Soc., 1995, 117, 1422–1427.
15. L. Echegoyen, F. Diederich and L.E. Echegoyen, Electrochemistry of Fullerenes, in Fullerenes: Chemistry, Physics, and Technology, Wiley, New York, 2000, 1.
16. H. Imahori, K. Hagiwara, T. Akiyama, M. Aoki, S. Taniguchi, T. Okada, M. Shirakawa and Y. Sakata, Chem. Phys. Lett., 1996, 263, 545‑550.
17. D.M. Guldi, Chem. Commun., 2000, 321‑327.

18. Teasdale, P.R.; Wallace, G.G. *Chimi Oggi*. 1992, 10: 19.
19. Riley, P.J.; Wallace, G.G. *J. Int. Mat. Syst. Struct.* 1991, 2: 228.
20. Wallace, G.G. *Mat. Forum* 1992, 16: 111.
21. Talaie, A.; Sadik, O.; Wallace, G.G. *J. Mat. Syst. Struct*. 1993, 4: 123.
22. Mirmohseni, R.; Price, W.E.; Wallace, G.G.; Zhao, H. *J. Int. Mat. Syst. Struct*. 1993, 4:43.
23. Honeybourne, C.L. *J. Phys. Chem. Solids* 1987, 48: 109.
24. Wirsen, A. *Electroactive Polymer Materials*. Technomic Publishing Co., Inc., Lancaster,1990.
25. Walton, D.J. *Mater. Design* 1990, 11: 142.
26. Genies, E.M. *Proceedings of European Physical Society*. Industrial Workshop, Lofthus, Norway, 1990: 93.
27. Kaner, R.B.; MacDiarmid, A.G. *Scientific Am.* 1988: 60.
28. Reynolds, J.R. *Chem. Tech*. 1988, 18: 440.
29. Kanatzidis, M.G. *Chem. Eng. News* 1990: 36.
30. L. Salem, The Molecular Orbital Theory of Conjugated Systems, Benjamin, New York, 1966.
31. A. Moliton, in: J.P. Goure (Ed.), Les sources de lumière, traité d'optoélectronique, Hermes, Paris, 2001.
32. M. Schott, C. R. Acad. Sci. Paris Sér. IV 1 (2000) 381.
33. D. Emin, in: T.A. Skotheim (Ed.), Handbook of Conducting Polymers, Vol. 2, M. Dekker, 1996, Chapter 26.
34. B. C. Thompson, J. M. J. Fréchet, Angew. Chem. Int. Ed. 47, 58 (2008).
35. M. A. Fox, M. Chanon, Photoinduced Electron Transfer – Part A: Conceptual Basis (Elsevier, Amsterdam, 1988).
36. P. W. M. Blom, V. D. Mihailetchi, L. J. A. Koster, D. E. Markov, Adv. Mater. 19, 1551 (2007).
37. X. Y. Zhu, Q. Yang, M. Muntwiler, Accounts Chem. Res. 42, 1779 (2009).
38. S. Günes, H. Neugebauer, N. S. Sariciftci, Chem. Rev. 107, 1324

(2007).
39. M. C. Scharber, D. Mühlbacher, M. Koppe, P. Denk, C. Waldauf, A. J. Heeger, C. J. Brabec, Adv. Mater. 18, 789 (2006).
40.R. Kroon, M. Lenes, J. C. Hummelen, P. W. M. Blom, B. De Boer, Polym. Rev.48, 531 (2008).
41. Y. F. Li, Y. P. Zou, Adv. Mater. 20, 2952 (2008).
42. S. H. Park, A. Roy, S. Beaupré, S. Cho, N. Coates, J. S. Moon, D. Moses, M. Leclerc, K. Lee, A. J. Heeger, Nat. Photonics 3, 297 (2009).
43. H. Y. Chen, J. H. Hou, S. Q. Zhang, Y. Y. Liang, G. W. Yang, Y. Yang, L. P. Yu, Y. Wu, G. Li, Nat. Photonics 3, 649 (2009).
44. E. G. Wang, L. T. Hou, Z. Q. Wang, S. Hellström, F. L. Zhang, O. Inganäs, M. R. Andersson, Adv. Mater. 22, 5240 (2010).
45. E. Verploegen, R. Mondal, C. J. Bettinger, S. Sok, M. F. Toney, Z. N. Bao, Adv. Funct. Mater. 20, 3519 (2010).
46. J. S. Kim, M. Granström, R. H. Friend, N. Johansson, W. R. Salaneck, R. Daik, W. J. Feast, F. Cacialli, J. Appl. Phys. 84, 6859 (1998).
47. G. A. Chamberlain, Solar Cells 8, 47 (1983).
48. C. W. Tang, Appl. Phys. Lett. 48, 183 (1986).
49. H. Spanggaard. F. C. Krebs, Sol. Energy Mater. Sol. Cells 83, 125 (2004).
50. M. F. Durstock, R. J. Spry, J. W. Baur, B. E. Taylor, L. Y. Chiang, J. Appl. Phys. 94, 3253 (2003).
51. L. A. A. Pettersson, L. S. Roman, O. Inganäs, J. Appl. Phys. 86, 487 (1999).
52. M. Hiramoto, H. Fujiwara, M. Yokoyama, Appl. Phys. Lett. 58, 1062 (1991).
53. C. J. Brabec, S. Gowrisanker, J. J. M. Halls, D. Laird, S. J. Jia, S. P. Williams, Adv. Mater. 22, 3839 (2010).
54. W. L. Ma, C. Y. Yang, X. Gong, K. Lee, A. J. Heeger, Adv. Funct. Mater. 15, 1617 (2005).

55. M. Reyes-Reyes, K. Kim, D. L. Carroll, Appl. Phys. Lett. 87, 083506 (2005).
56. G. Li, Y. Yao, H. C. Yang, V. Shrotriya, G. W. Yang, Y. Yang, Adv. Funct. Mater. 17, 1636 (2007).
57. M. Campoy-Quiles, T. Ferenczi, T. Agostinelli, P. G. Etchegoin, Y. Kim, T. D. Anthopoulos, P. N. Stavrinou, D. D. C. Bradley, J. Nelson, Nat. Mater. 7, 158 (2008).
58. M. S. Kim, J. S. Kim, J. C. Cho, M. Shtein, L. J. Guo, J. Kim, Appl. Phys. Lett. 90, 123113 (2007).
59. C. F. Shih, K. T. Hung, J. W. Wu, C. Y. Hsiao, W. M. Li, Appl. Phys. Lett. 94, 143505 (2009).
60. J. Y. Kim, S. H. Kim, H. H. Lee, K. Lee, W. L. Ma, X. Gong, A. J. Heeger, Adv. Mater. 18, 572 (2006).
61. H. L. Yip, S. K. Hau, N. S. Baek, H. Ma, A. K. Y. Jen, Adv. Mater. 20, 2376 (2008).
62. D. H. Ko, J. R. Tumbleston, L. Zhang, S. Williams, J. M. DeSimone, R. Lopez, E. T. Samulski, Nano Lett. 9, 2742 (2009).
63.E. von Hauff, J. Parisi, V. Dyakonov, Thin Solid Films 511-512, 506 (2006).
64. M. A. Green, K. Emery, Y. Hishikawa, W. Warta, and E. D. Dunlop, Prog. Photovolt: Res. Appl. 19, 565 (2011).
65. S. Choi, W. J. Potscavage, B. Kippelen, J. Appl. Phys. 106, 054507 (2009).
66. S. Y. Park, W. I. Jeong, D. G. Kim, J. K. Kim, D. C. Lim, J. H. Kim, J. J. Kim, J. W. Kang, Appl. Phys. Lett. 96, 173301 (2010).
67. T. Ameri, G. Dennler, C. Waldauf, H. Azimi, A. Seemann, K. Forberich, J. Hauch, M. Scharber, K. Hingerl, and C. J. Brabec, Adv. Funct. Mater. 20, 1592 (2010).
68. S. I. Na, S. S. Kim, J. Jo, and D. Y. Kim, Adv. Mater. 20, 4061 (2008).
69. A. L. Ayzner, C. J. Tassone, S. H. Tolbert, B. J. Schwartz, J. Phys.

Chem. C 113, 20050 (2009).
70.K. H. Lee, P. E. Schwenn, A. R. G. Smith, H. Cavaye, P. E. Shaw, M. James, K. B. Krueger, I. R. Gentle, P. Meredith, P. L. Burn, Adv. Mater. 23, 766 (2011).
71. J. S. Moon, C. J. Takacs, Y. M. Sun, A. J. Heeger, Nano Lett. 11, 1036 (2011).
72. Kessler MR, Sottos NR, White SR. Composites, Part A 2003;34:743‑53.
73. Currey JD, New Jersey: Princeton University Press; 2002.
74. Gibson LJ, Ashby MF, Harley BA, Cambridge: Cambridge University Press; 2010.
75.Tirrell M, editor, Washington (DC): The National Academies Press; 1994 [NMAB-464].
76.Buehler MJ, Keten S, Ackbarow T, Prog Mater Sci 2008;53:1101‑241.
77.Mayer G, Science 2005;310:1144‑7.
78.Gordon JE, New York: W.H. Freeman and Company; 1988. p. 98.
79. Ma M, Vijayan K, Hiltner A, Baer E, Im J, J Mater Sci 1990;25:2039‑46.
80. Ma M, Im J, Hiltner A, Baer E, J Appl Poly Sci 1990;40:669‑84.
81.Syn CK, Lesuer DR, Wolfenstine J, Sherby OD, Mater Trans A 1993;24:1647‑53.
82.Ortiz C, Boyce MC, Science 2008;319:1053‑4
83. Aizenberg J, MRS Bull 2010;35:323‑30.

Chapter 2

Preparation and photoelectric properties of C60- poly(ethylene glycol) and poly(3,4-ethylenedioxythiophene) composite gel by low-temperature organic-solvents processed

Abstract

C60 fullerene derivatives, formed by grafting of polymer chains onto C60 fullerene, can improve its solubility in solvents. And they were able to composite with various functional polymers to form interpenetrate network structures gel. In this study, a composite gel of C_{60} fullerene derivatives and poly(3,4-ethylenedioxythiophene)(PEDOT) was prepared by low-temperature organic-solvents processed, and its photoelectric properties were evaluated. Herein, poly(ethylene glycol)(PEG) radicals were successfully trapped on fullerene (C_{60}) which worked as a cross-linking point to give C_{60}-PEG gel, and PEDOT using chemical oxidative polymerization was composited with it, formed C_{60}-PEG/PEDOT gel. The structure of the film using this composite material was identified. From the result, C_{60}-PEG/PEDOT film has amorphous network structure, and the UV response was much higher than C_{60}-PEG gel, it was estimated that PEDOT was synthesized inside of C_{60}-PEG gel and was able to form nanoscale junction between C_{60} and PEDOT, which was beneficial to the movement of electrons and holes. The photocurrent was observed by irradiating with UV or simulated sunlight on an electrode of C_{60}-PEG/PEDOT gel, power conversion efficiency (PCE) was calculated as 1.2×10^{-3}%, so it was expected that C_{60}-PEG/PEDOT material can be applied to photoelectric translation field such as solar cells.

2.1 Introduction

During approximately 20 years, attentions have been paid for C_{60} fullerene [1-3] for its attractive physical and chemical properties. For example, the ability to accept and release electrons, [4, 5] the ability to trap free radical,[6] physiological activity,[7] and photo-activity, [8] etc. But before those properties, the interaction of C60 with light has attracted considerable interest in the applications, for instance, solar cells, [9-11] related to photochemical and photo-induced charge transfer properties of C60 derivatives.[12] Its remarkable electrochemical properties, with six reversible single-electron reduction waves,[13] have aroused the hope of a successful use in many fields, such as biological [14-16] and polymeric material, [17-20]etc.

However, the solubility of C_{60} fullerene in most solvent [21] was very poor, which stood in the way of C_{60} fullerene's wide applications. For solving this problem, from basic research to developed application, various methods had been reported, [22, 23] one was grafting of polymer chains onto C_{60} fullerene,[24] because not only it can improve the solubility of C_{60} fullerene to form a homogeneously dispersed solution, but can also enhance some properties for the new network structure materials.[25-28]

We have reported that PEG radicals formed by the thermal decomposition of macro azo-initiator, Azo-PEG_2, [29-31] were successfully trapped on C_{60} fullerene surface and a C_{60} worked as a cross-linking point giving C_{60}-PEG gel, which formed network structure.

In this paper, we focused on photo-activity of C_{60} device which play important role as solar cell with PEDOT. Preparation of C_{60}-PEG gel with PEDOT under low-temperature by organic-solvents processed was demonstrated. C_{60}-PEG gel was composed with PEDOT which was synthesized by chemical oxidative polymerization. The structure of C_{60}-PEG/PEDOT gel was identified by scanning electron microscope (SEM), Fourier transform infrared (FT-IR) spectroscopy, x-ray diffraction (XRD). At last, the photoelectric property of composite gel was evaluated.

2.2 Experimental

2.2.1 Materials and reagents

The C_{60} fullerene used was "nanom purple N60-ST", obtained from Frontier Carbon Corporation Co., Ltd., which was used without further purification. The purity was greater than 96% and average particle size was 30-70μm. C_{60} fullerene was dried in vacuum at 50 °C before use. Its chemical structure and properties were shown in Figure 2-1and Table 2-1, respectively.

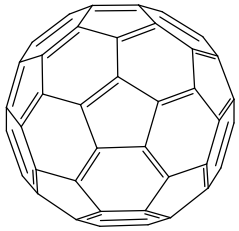

Figure 2-1 Chemical structure of buckminsterfullerene (C_{60}).

Table 2-1 Properties of C_{60}, nanom purple ST

Purity (%)	Average particle size (μm)	Bulk density (g/cm^3)
> 96	30−70	0.63

Macro azo-initiator, $(Azo\text{-}PEG)_n$, was commercially obtained from Wako Pure Chemical Industries, Ltd, Japan (commercial name of the $(Azo\text{-}PEG)_n$ was VPE-0201). The molecular weight of PEG unit was $2.0x10^3$ and it contains several azo groups, which can form polymer radical. Its chemical structures was shown in Figure 2-2.

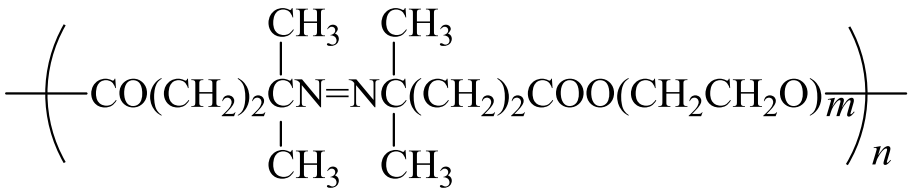

Figure 2-2 Chemical structures of polyethylene glycol macroazoinitiators

(Azo-PEGs), VPE series (Wako Pure Chemical Industries, Ltd.)

3,4-ethylendioxythiophene (EDOT) obtained from Sigma Aldrich Co., LLC., which was used without further purification.
3,4-ethylendioxythiophene (EDOT) obtained from Sigma Aldrich Co., LLC. was used without further purification. The chemical structure of EDOT is shown in Figure 2-3.

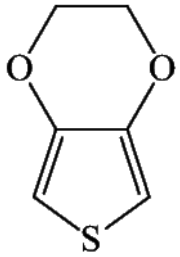

Figure 2-3 chemical structure of EDOT

2.2.2 Reaction of C_{60} fullerene and $(Azo\text{-}PEG)_n$

A typical preparing method of C_{60}-PEG gel network is as follows. 5.0 x 10^{-2} g (6.9 x 10^{-5} mol) of C_{60} fullerene, 0.70 g (PEG unit 3.5 x 10^{-4} mol) of $(Azo\text{-}PEG)_n$, and 20.0 mL of toluene were blended in a glass tube, degassed with several freeze-thaw cycles, and sealed off under high vacuum using sealed tubes. Then the sealed tubes were heated at 70 °C under the condition of stirring. After 12 hours, excess toluene was removed using a centrifugal evaporator (Scheme 2-1), then C_{60}-PEG sol was prepared, dropped it onto ITO glass, after drying at 60 °C for three days, C_{60}-PEG gel was prepared.

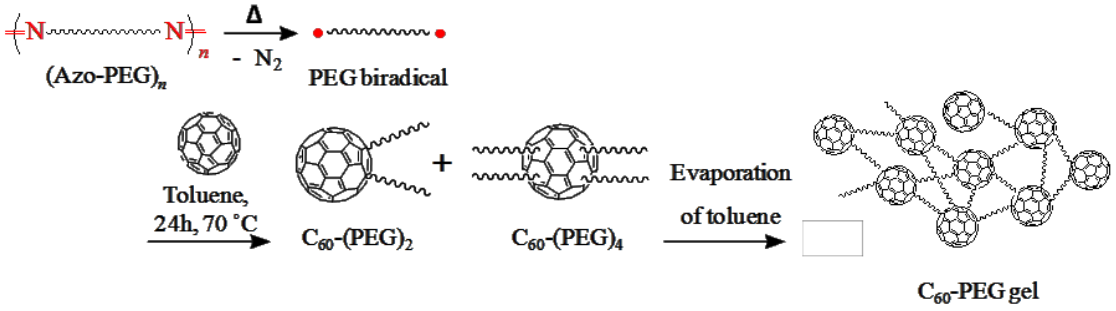

Scheme 2-1 Reaction of C_{60} fullerene and $(Azo\text{-}PEG)_n$

2.2.3 Preparation of C_{60}-PEG/PEDOT gel

Before C_{60}-PEG sol was prepared, $FeCl_3$ was used as an oxidative agent and EDOT/$FeCl_3$ solution was prepared by mixing EDOT and $FeCl_3$ in toluene. Then EDOT/$FeCl_3$ solution was added into C_{60}-PEG gel, and dropped this gel onto ITO glass, after drying at 60°C for three days, C_{60}-PEG/PEDOT gel was prepared.

PEDOT was synthesized by chemical oxidative polymerization. $FeCl_3$ was dissociated to Fe^{3+} and $3Cl^-$ in EDOT/$FeCl_3$ toluene solution. Once EDOT and Fe^{3+} contacted, the polymerization of EDOT was initiated by moving an electron from EDOT to Fe^{3+}. EDOT works as an active center and was added to another EDOT molecule. This process was repeated many times and PEDOT was obtained (Scheme 2-2).

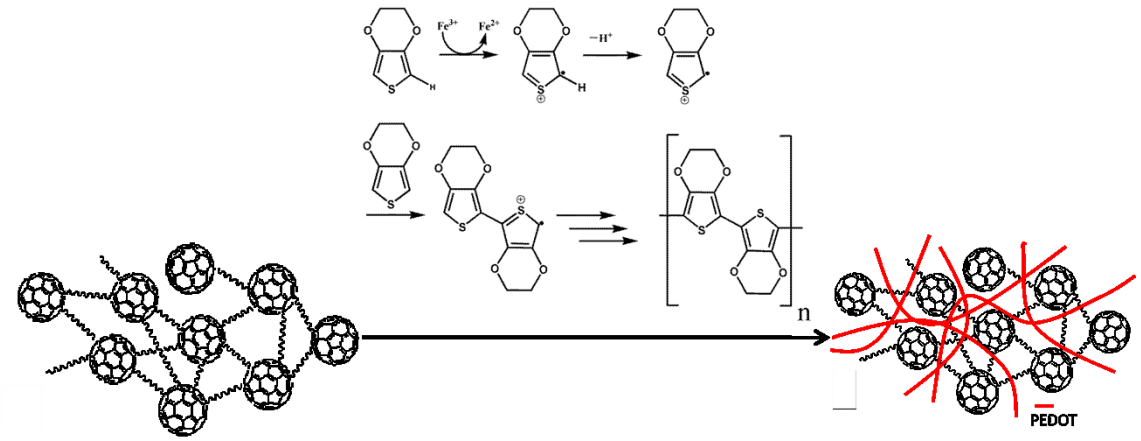

Scheme 2-2 Synthesis of PEDOT by chemical oxidative polymerization

2.2.4 Fabrication process of polymer solar cells device

C60-PEG/PEDOT gel was evaporated by rotary evaporation under the condition of 40 Degrees Celsius, 50mmHg (millimeter mercury), then this gel was coated onto ITO glass using spin-coater at 1000-2500rpm (revolutions per minute). After 30s, active layer film was ready. Then, this

film was dried at 60 degrees Celsius for 72 hours. The C60-PEG/PEDOT film was obtained. The process was shown in Figure2-4.

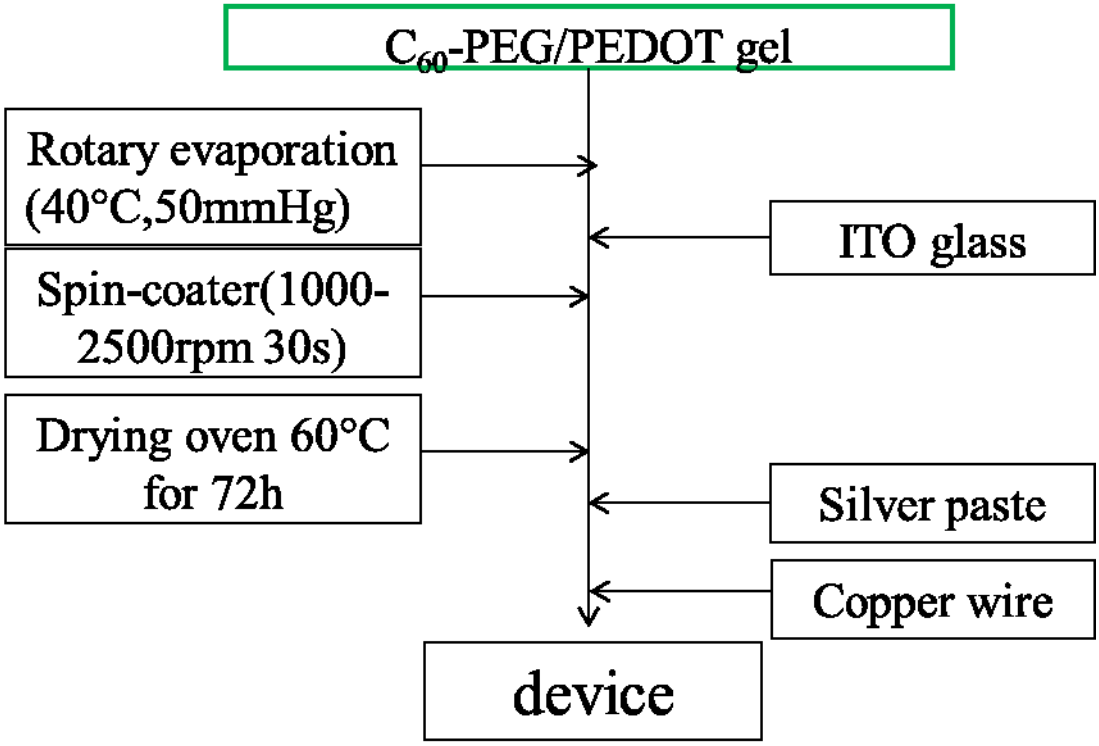

Figure2-4 Fabrication process of photovoltaic device of polymer solar cells

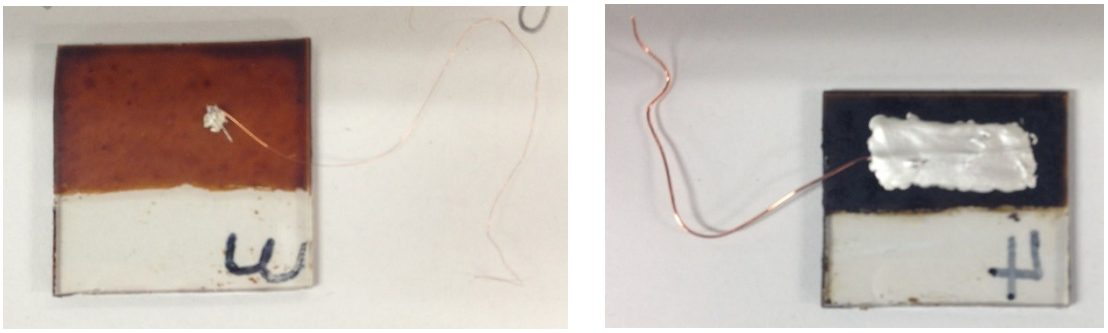

Figure2-5 The electrodes of photovoltaic device of polymer solar cells

2.2.5 Measurement

For measuring the characteristic of the composited gel, C60-PEG/PEDOT gel was dried to make a C60-PEG/PEDOT film.

Scanning electron microscope (SEM) of the gel surface and cross section was carried out on a SEM (JSM-6510, JEOL, Ltd.) at an acceleration voltage

of 5 kV.

Infrared spectra were recorded on a FT-IR spectrophotometer, Shimazu Manufacturing Co., Ltd. FTIR-8400S.

XRD was recorded with a Rigaku Co., Ltd. RINT2100 made using 0.2 mm thick sample plates, the measurement wavelength went at 1.54 nm.

2.2.6 Photoelectric properties

C_{60}-PEG gel and C_{60}-PEG/PEDOT gel were connected with copper line by Ag paste respectively, and connected to digital multi-mater (Advantest Co., Ltd. R6871E-DC). UV lamp (Wavelength at 365nm) was set onto the gels which was irradiated for each 5 min under 20^{o}C, 65 % humidity and the resistance was measured during this process (Figure 2-6). Electro conductivity was calculated by resistance, thickness, width and length of the gel.

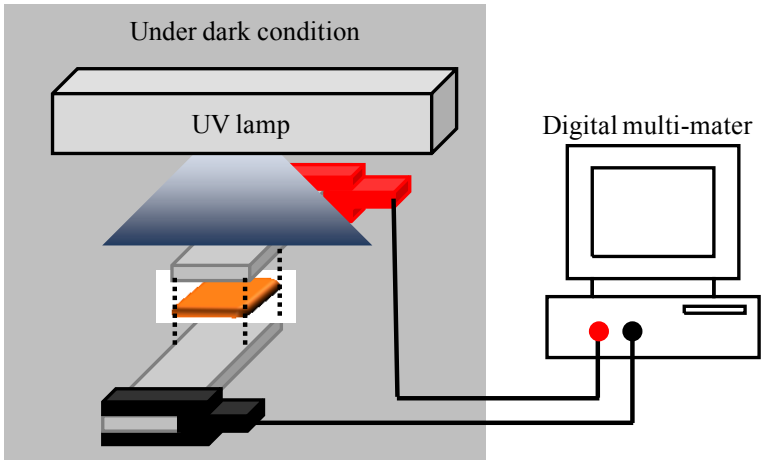

Figure 2-6 Schematic illustration of UV response measurement

2.2.7 Power conversion efficiency

Power conversion efficiency (PCE) of C_{60}-PEG/PEDOT film device was investigated. The devices were fabricated using C_{60}-PEG/PEDOT gel which was connected with copper line by Ag paste. Photocurrent was measured when voltage applied from - 1.0 V to 1.0 V by irradiating a solar simulator (HAL-C100, 100 W compact xenon light source, ASAHI

SPECTRA) with AM1.5G spectra at 100 mW cm^{-2} at room temperature(Figure 2-7). Dark current was measured under the same conditions without simulated sun light.

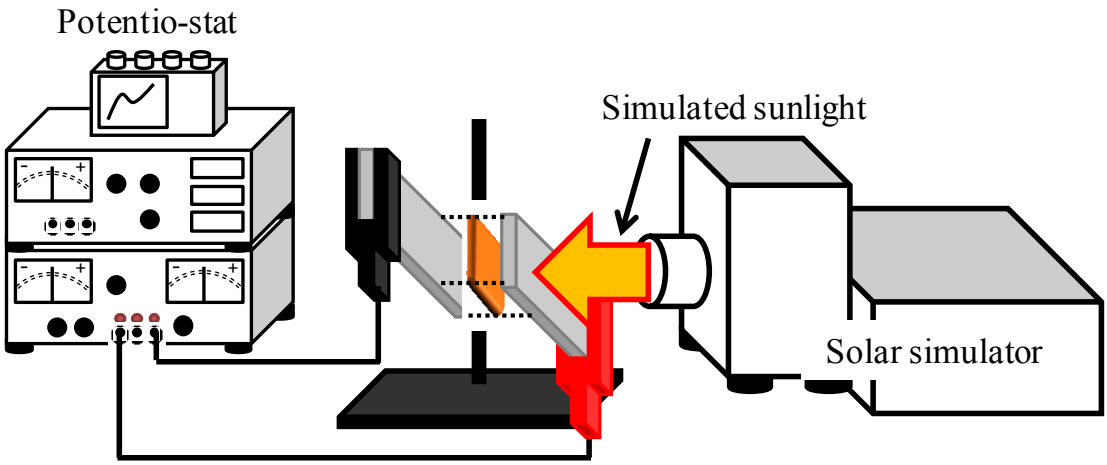

Figure 2-7 Schematic illustration of PCE measurement

2.3 Results and Discussion

2.3.1 Preparation of C60-PEG/PEDOT composite gel

C_{60}-PEG gel electrode was prepared by casting C_{60}-PEG sol onto ITO electrode. PEDOT was synthesized inside of C_{60}-PEG gel by dropping $FeCl_3$/EDOT solution. C_{60}-PEG gel and PEDOT formed C_{60}-PEG/PEDOT gel, a composite material which has network structure. Comparing C_{60}-PEG gel with C_{60}-PEG/PEDOT gel prepared by chemical oxidative polymerization under low-temperature organic-solvents processed, found C_{60}-PEG gel has flat surface and the brown color and the surface of C_{60}-PEG/PEDOT gel has asperity and its color slightly changed from brown to dark brown caused by PEDOT, and the film of C_{60}-PEG/PEDOT were flexible and elastic film that can be processed easily (Figure 2-8).

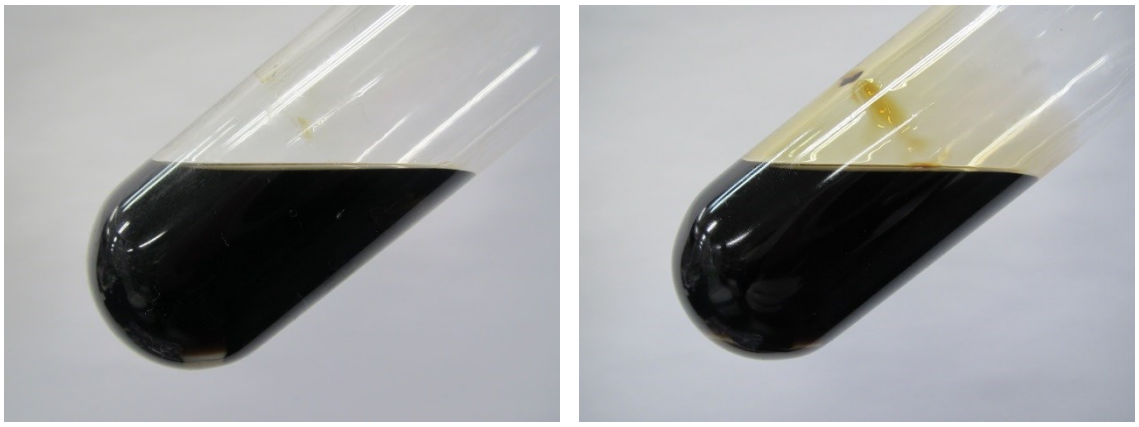

Figure 2-8 Photographs of C_{60}-PEG gel and C_{60}-PEG/PEDOT gel

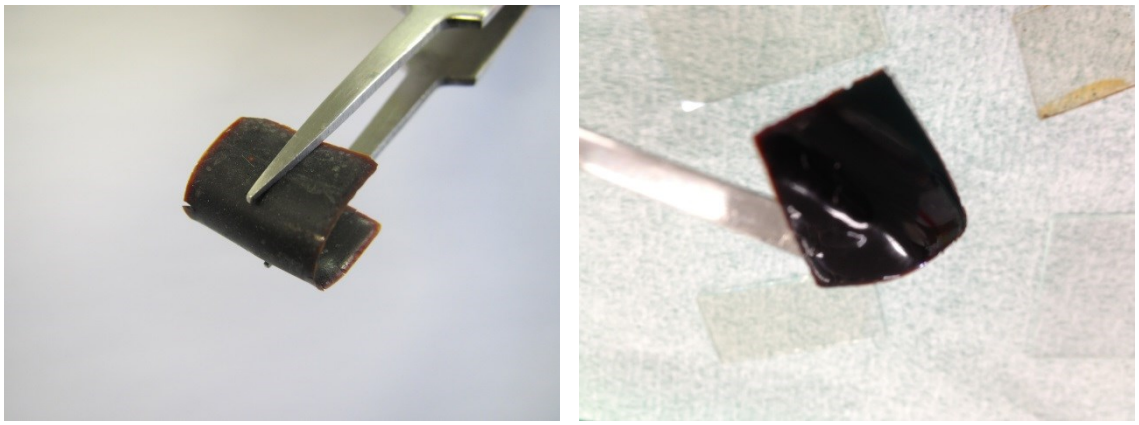

Figure 2-9 Photographs of C_{60}-PEGfilm and C_{60}-PEG /PEDOT film

2.3.2 The morphology of C60-PEG /PEDOT film

The morphologies of C_{60}-PEG/PEDOT films were observed utilizing SEM, three kinds of different resolution SEM image of C_{60}-PEG/PEDOT films surface were shown in Figure 2-9. Porous structures of C_{60}-PEG/PEDOT composite materials were confirmed from figure 2-9 b, it was considered that the porous structure of this material were formed from the solvents evaporation, after evaporated toluene, lots of porous cells were formed at the spaces between C_{60}-PEG and PEDOT. It can be observed from the cross section of polymer solar cells device using C_{60}-PEG/PEDOT gel as active layer again.

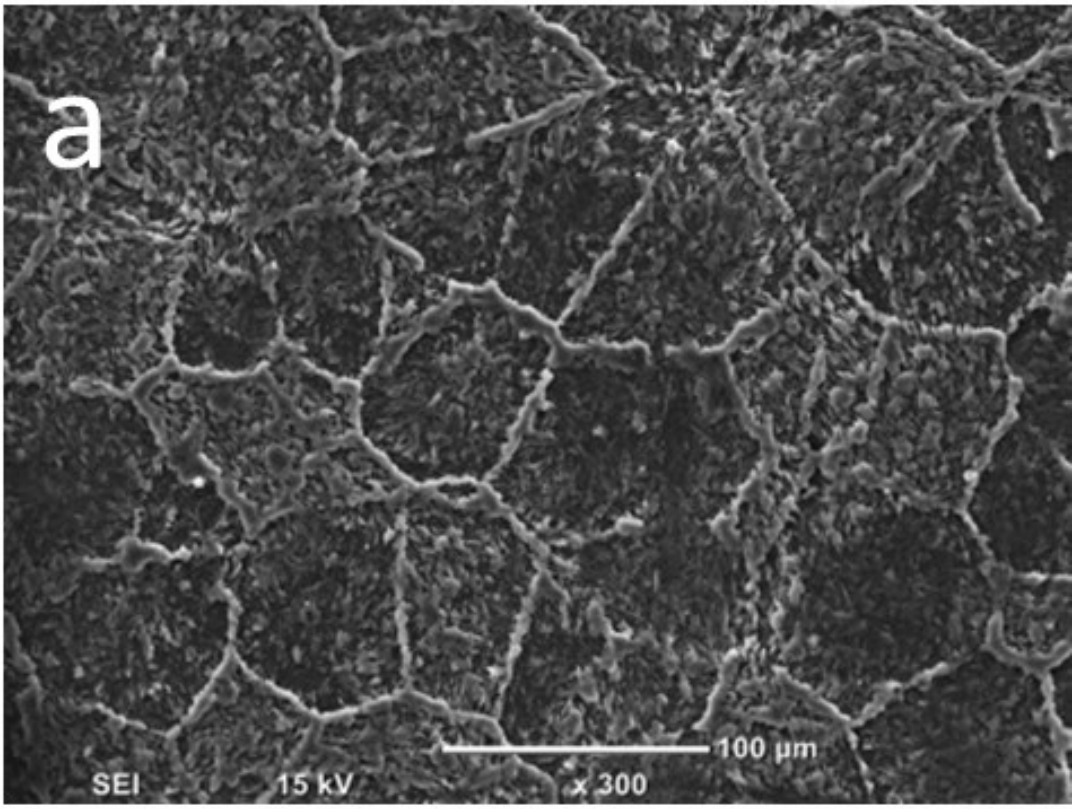

100 µm

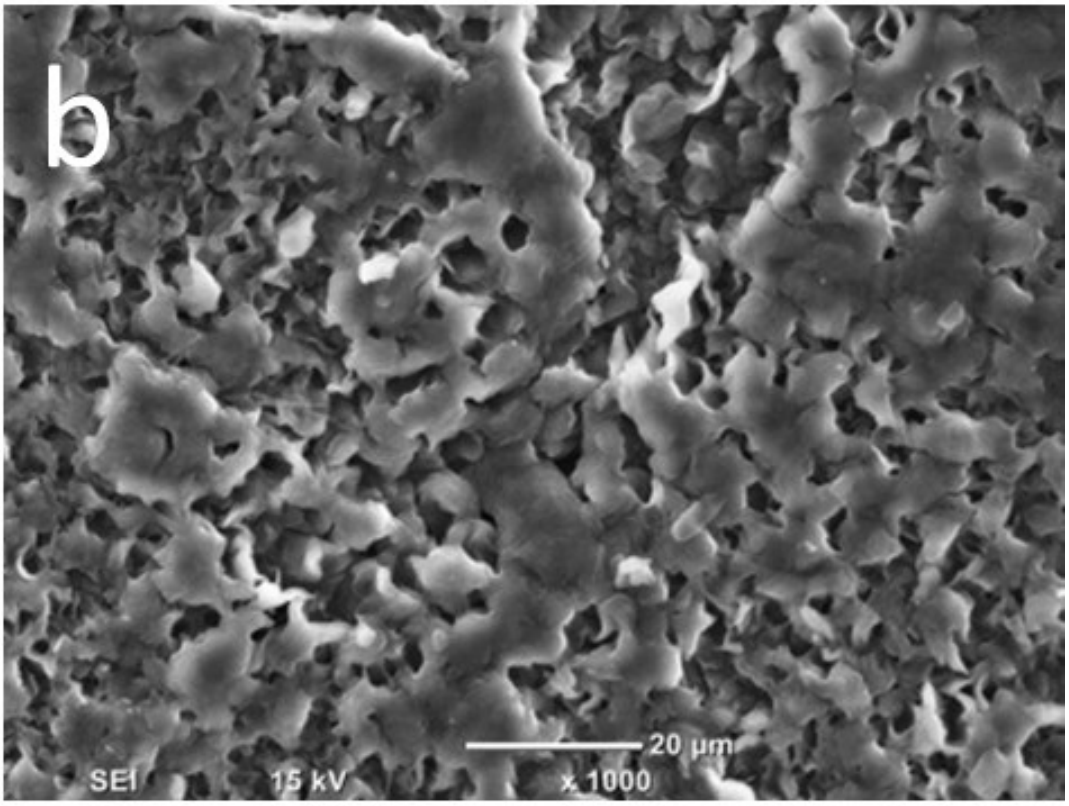

Figure 2-9 SEM micrographs of C60-PEG/PEDOT films: (a) surface of film, scale bar 100 μm (b)porous surface of film, scalebar 20 μm

2.3.3 FT-IR spectrum

Figure 2-10 shows FT-IR spectra of (a) C_{60}-PEG gel, (b) PEDOT and (c) C_{60}-PEG/PEDOT gel. The spectrum of (a) C60-PEG gel showed characteristic absorptions of PEG at 2925 and 1110 cm^{-1}, which is characteristic of -CH2- and -O-, respectively. From these results, it is considered that PEG biradicals were trapped by C60 fullerene to give C60-PEG gel having C60 fullerene at cross-linking point.

In the spectrum of C60-PEG/PEDOT, there are characteristic absorptions of methylene at 2925 cm^{-1} and enoxy at 1105 cm^{-1}, which are from C60-PEG gel; and there are characteristic absorptions of thiophene at

1520 and720 cm^{-1}, which are from PEDOT. It was considered that PEG biradicals were trapped by C60 fullerene successfully, C60 fullerene at cross-linking point, and PEDOT was synthesized into C60-PEG film to form interpenetrate network structure composite material.

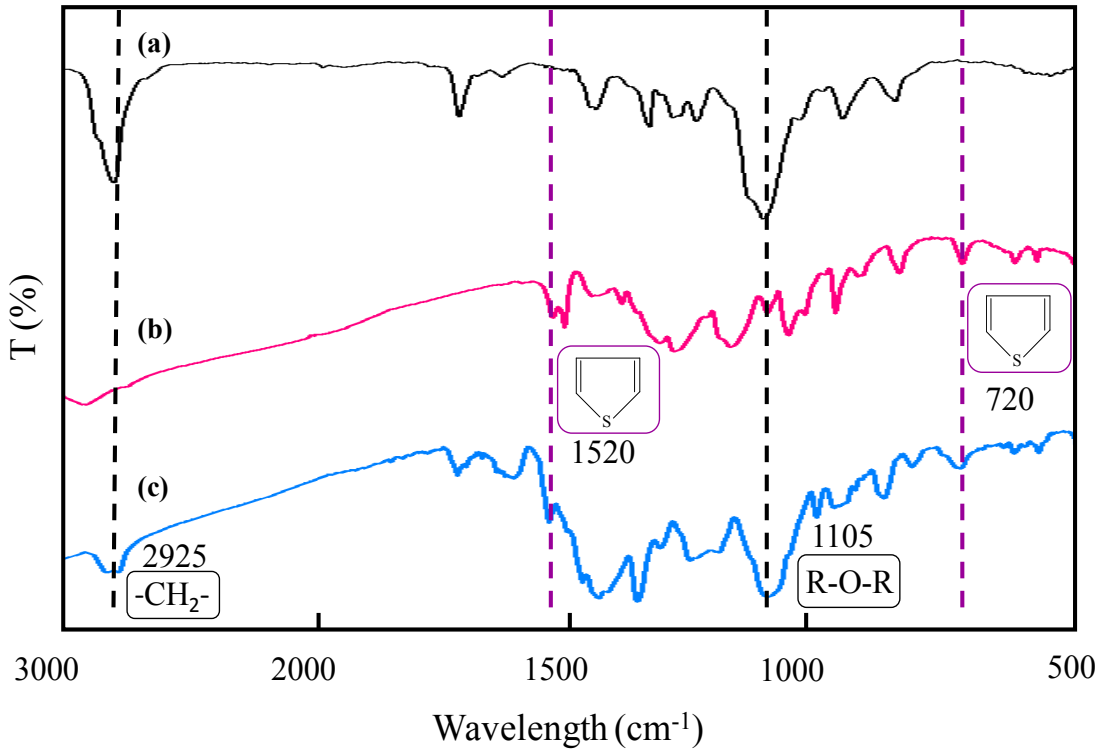

Figure 2-10 FT-IR spectra of (a) drying C60-PEG gel (b) PEDOT and (c) drying C60-PEG/PEDOT gel

2.3.4 Crystalline structure of two gels

Figure 2-11 shows XRD patterns of (a) C_{60}-PEG gel, (b) C_{60}-PEG/PEDOT gel. C_{60}-PEG gel has broad peak on 15 to 25 degree and double sharp peaks on the broad peak. C_{60}-PEG/PEDOT gel has broad peak on 15 to 25 degree as same as C_{60}-PEG gel. However, sharp peaks were not observed in C_{60}-PEG/PEDOT gel. It was considered that C_{60}-PEG gel has crystalline structure because they had sharp peaks. On the other hand, C_{60}-PEG/PEDOT gel dispersed the sharp peaks, It was suggested that prepared C_{60}-PEG/PEDOT gel has amorphous structure and it was composited on molecule scale.

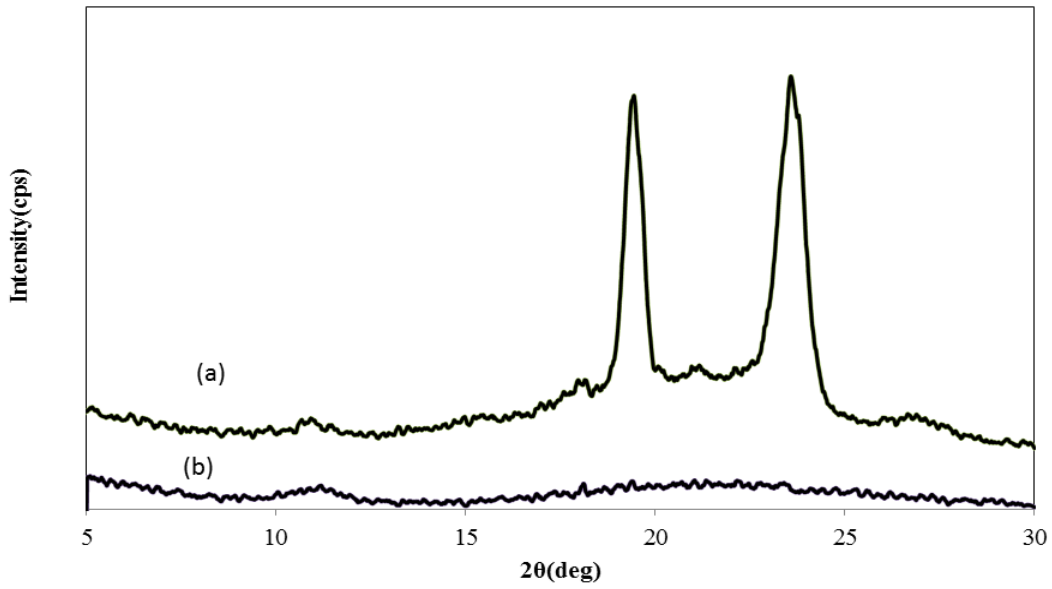

Figure 2-11 XRD patterns of (a) C60-PEG gel and (b) C60-PEG/PEDOT gel

2.3.5The structure of devices of polymer solar cells

The device structure was shown in Figure 2-12a (starting from the bottom: glass/ITO, C_{60}-PEG/PEDOT photoactive layer, with a final Ag electrode). The top-view scanning electron microscopy of C_{60}-PEG/PEDOT film on ITO glass was just as previously showed (Figure2-8). Figure 2-12b was shown the cross-section scanning electron microscopy. The results reveal that the C_{60}-PEG/PEDOT film was uniform despite on ITO glass, and the surface appears smooth. The cross-section SEM image of devices without the Ag electrode shown in Figure 4b show a well-defined layer-by-layer structure with sharp interfaces, and there were lots of holes into active layer, it was just as previously discussed, it was estimated the microstructure of active layer was interpenetrate network structure, after drying the structure material, toluene (as solvent in the space of the structure) was evaporated, and holes were kept back into active layer surface and inside. The thickness of active layer was about 33.3μm.

Here, the thickness of C_{60}-PEG/PEDOT layer was sufficient to serve as the light-absorbing layer. Moreover, charge extraction from the photoactive layer to electrodes was still efficient due to the long carrier lifetime and good carrier transport properties. C_{60}-PEG/PEDOT film was able to ensure sufficient light absorption, which was the first decisive factor for photoelectric conversion performance.

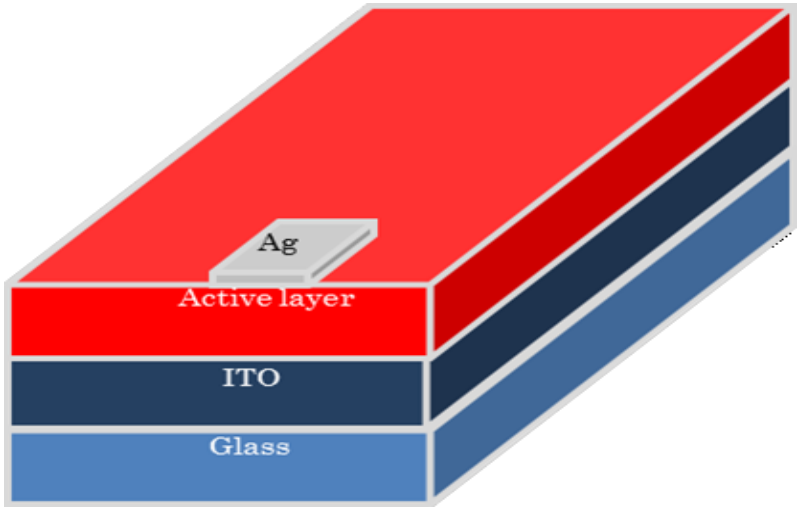

(a)

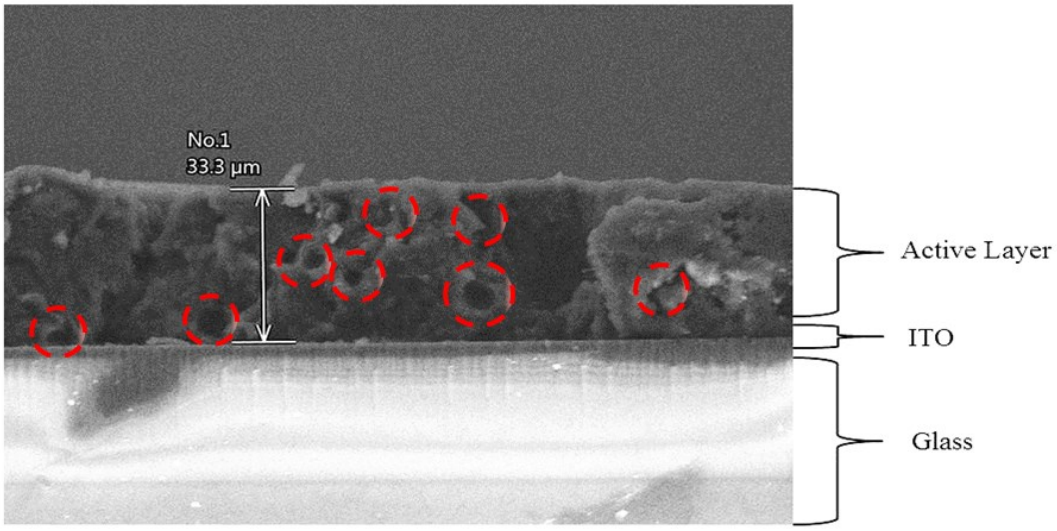

(b)

Figure 2-12 Device structure of low-temperature processed polymer solar cells. From the bottom: glass/ITO/ C60-PEG/PEDOT/Ag, the cross section of the device except for the Ag electrode. The thickness of active layer was 33.3μm.

2.3.6 UV response of C_{60}-PEG/PDOT film

Figure 2-13 shows UV response of C_{60}-PEG/PDOT film. Once the film was UV irradiated, electro conductivity was increased rapidly to reach constant value. Without UV irradiation, electro conductivity was decreased rapidly.

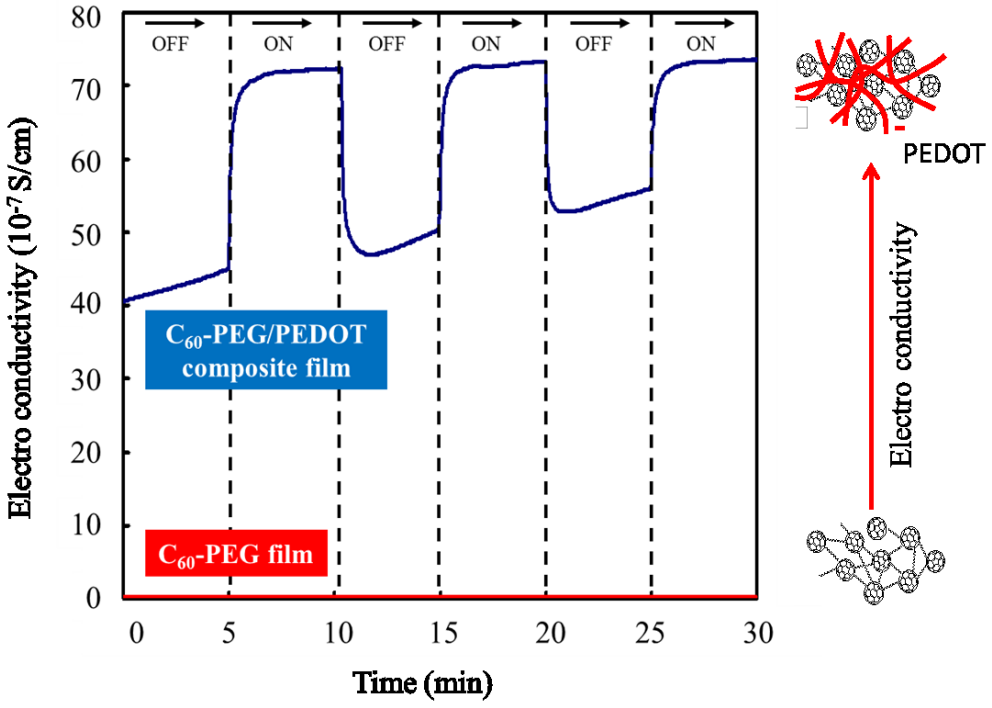

Figure 2-13 UV response of C60-PEG film and C60-PEG/PEDOT film prepare by chemical oxidative polymerization.

The conductivity of C60-PEG film was increased from 2.96 x 10^{-11} (S/cm) to 1.79 x 10^{-9}(S/cm), and the conductivity of C60-PEG/PEDOT film was increased from 2.11 x 10^{-6} (S/cm) to 6.05 x 10^{-6}(S/cm), respectively. It was considered that conductivity was increased because the electron in

π-conjugated system of C_{60} moved faster when C_{60}-PEG/PEDOT gel was UV irradiated. It has much higher response compared with C_{60}-PEG gel because PEDOT was synthesized inside of C_{60}-PEG gel. It was estimated that nanoschale junctions were formed between C_{60} and PEDOT. When UV irradiated, C_{60} worked as n-type semiconductor and PEDOT worked as p-type semiconductor and electro conductivity of C_{60}-PEG/PEDOT gel was increased by moving electron from C_{60} to PEDOT.

2.3.7 UV-Vis absorption spectra

Figure 2-14 shows UV-Vis absorption spectra of C60-PEG and C60-PEG/PEDOT.C60-PEG and C60-PEG/PEDOT show an absorption maximum(λ_{max}) wavelength at 326nm and 335nm, respectively, Which are from the π-π* transition of the conjugated system. The peak of C60-PEG/PEDOT shows significantly redshift from the peak of C60-PEG material. It was estimated that such red shift was attributed to bandgap narrowing, so we calculated the bandgap of C60-PEG material and C60-PEG/PEDOT material(shown in Table 2-2). The absorption edges of C60-PEG and C60-PEG/PEDOT are at 444nm and 470nm, respectively. The optical bandgap ($E_{g,opt}$) for C60-PEG and C60-PEG/PEDOT are 2.79eV and 2.64eV, respectively. The result shows that the bandgap of C60-PEG/PEDOT material is smaller than C60-PEG materials, that is, C60-PEG/PEDOT material is stronger absorption of UV light than C60-PEG material.

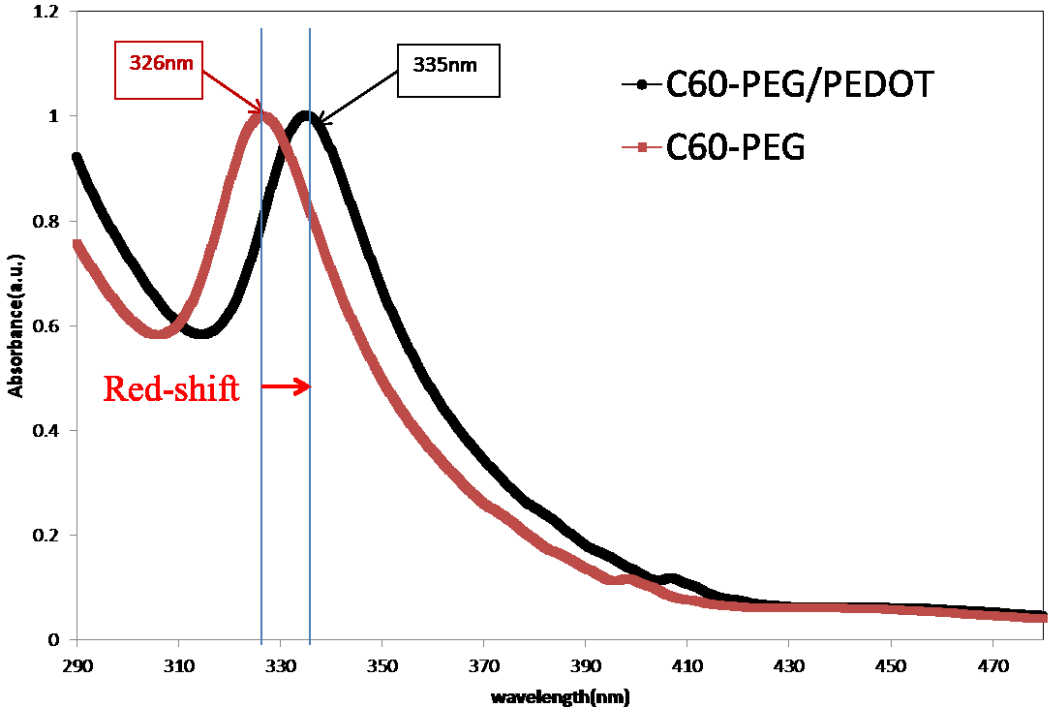

Figure 2-14 UV-Vis absorption spectra of C60-PEG material and C60-PEG/PEDOT material

Table 2-2 The bandgap of C60-PEG and C60-PEG/PEDOT

Material	λ_{max} [nm]	λ_{edge} [nm]	[a)]$E_{g,OPT}$ [eV]
C60-PEG	326	444	2.79
C60-PEG/PEDOT	335	470	2.65

[a)]$E_{g,OPT}=1240/\lambda_{edge}$

2.3.8 Photovoltaic property of polymer solar cells device

We have achieved device performance on the basis of low-temperature (less than 70℃) organic processed polymer solar cells, advising that it was possible to get device performance of flexible polymer solar cells base on the processing techniques utilized. A photograph of the flexible active layer was shown in Figure 6a, and the current density-voltage curve of C60-PEG/PEDOT device was shown in Figure 2-15 b. Photocurrent was measured when voltage applied from - 1.0 V to 1.0 V by irradiating a solar

simulator (HAL-C100, 100 W compact xenon light source, ASAHI SPECTRA) with AM1.5G spectra at 100 mW cm^{-2} at room temperature. On photo current, under simulated sunlight irradiation, the C60-PEG/PEDOT heterojuction solar cell device shows a classic polymer solar cells photovoltaic property with a short-circuit current Jsc of 0.02mA/cm^2, an open-circuit voltage Voc of 0.16V, fill factor FF of 42.26, and PCE η(%) of 1.2×10^{-3} . The loss in PCE arises from the decreased Jsc and Voc, which could result from too smooth surface and thick thickness of the active layer, which could be solved in the near future by surface modified using to mimic the unique functionalities of biological systems for practical applications, such as antireflection and antiglaring of moth eye microstructure.

From these results, photo current was observed from C_{60}-PEG/PEDOT device. However, it was not observed in C_{60}-PEG device and simple layer stack of C_{60}-PEG gel and PEDOT device. Thus it was considered that PEDOT and C_{60}-PEG were contacted in nano-schale to form bulk heterojunction polymer solar cells with interpenetrate network structure, which was able to transfer the electron and hole efficiently. Photo current of simple layer stack of C_{60}-PEG gel and PEDOT was not observed because C_{60} and PEDOT were contacted only at the interface and it was difficult to transfer electron and hole.

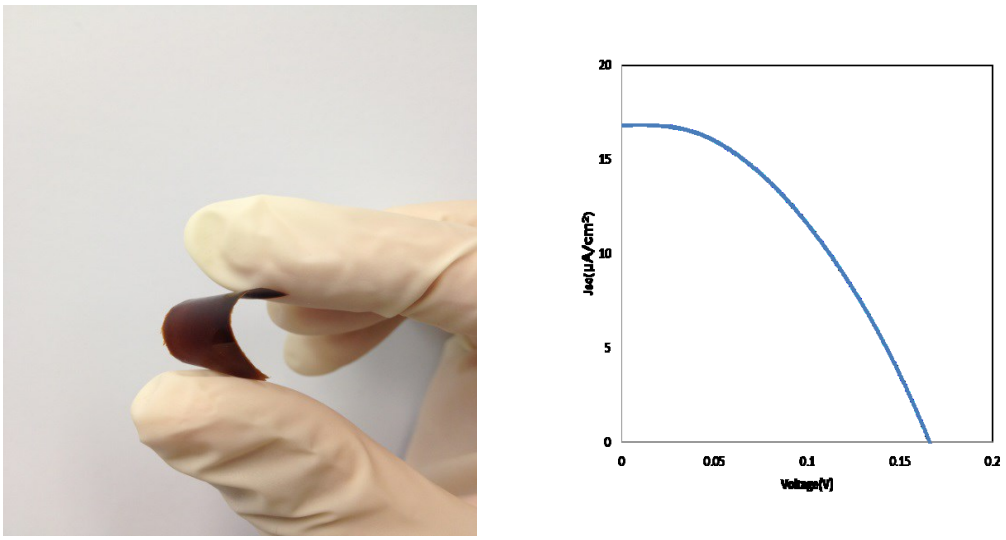

(a) (b)

Figure 2-15 (a) Photo image of flexible C60-PEG/PEDOT film and (b) Current density-voltage curves of C60-PEG/PEDOT heterojunction solar cell under illumination.

Table 2-3 shows the photoelectrical properties of polymer solar cell devices using C60-PEG/PC material and C60-PEG/PEDOT material. PCE of the devices using C60-PEG/Pc (Phthalocyanine) material is refered to Master Thesis of Hideaki Takahashi. From this table, the short circuit current of C60-PEG/PEDOT device is more 10 times higher than C60-PEG/Pc device, because the interpenetrate network structure is convenient to the charge carriers transport. It is estimated that PEDOT is not only a good conductive polymer material but a good P-type semiconductor material.

Table 2-3 Photoelectrical properties of devices using different material under 100 mW/cm^2 AM1.5G of simulated solar illumination at room temperature

P-type	Material	J_{SC} (μA/cm^2)	V_{OC} (V)	FF	PCE (%)
	[a]C60-PEG/H_2Pc	0.79	1.24	0.48	4.7×10^{-4}
	[a]C60-PEG/CuPc	0.80	1.21	0.41	4.0×10^{-4}
	[a]C60-PEG/ZnPc	0.10	0.17	0.35	6.0×10^{-6}
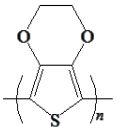	[b]C60-PEG/PEDOT	1.4	0.18	0.57	1.14×10^{-4}
	[b]C60-PEG/PEDOT	16.8	0.17	0.42	1.16×10^{-3}
	[b]C60-PEG/PEDOT	10.4	0.20	0.75	1.58×10^{-3}

Table 2-4 shows the data of PCE changing with the molar ratio of C60 and PEG. Obviously the increase of C60 in the polymer mixture has a positive effect on PCE, however, when the molar ratio of C60 to PEG is more than 1:4, it has a negative effect on PCE, under the same condition, the film flexibility turns bad . In here, the molar ratio of C60 to PEG has been optimized to approximately 1:4.the best PCE is 1.6 times ten to power minus three.

Table 2-4 Data of PCE changing with the molar ratio of C60 and PEG

NO.	**Molar ratio**		**Weight (mg)**		**EDOT(ml)**	**$FeCl_3$(ml)**	**PCE(%)**
	C60	PEG	C60	PEG	$\times10^{-2}$		$\times10^{-3}$
1	1	5	50	700	2.9	7.35	0.0005
2	1	4.5	56	700	2.9	7.35	1.1681
3	1	4	62	700	2.9	7.35	1.5896
4	1	3.7	68	700	2.9	7.35	0.1408

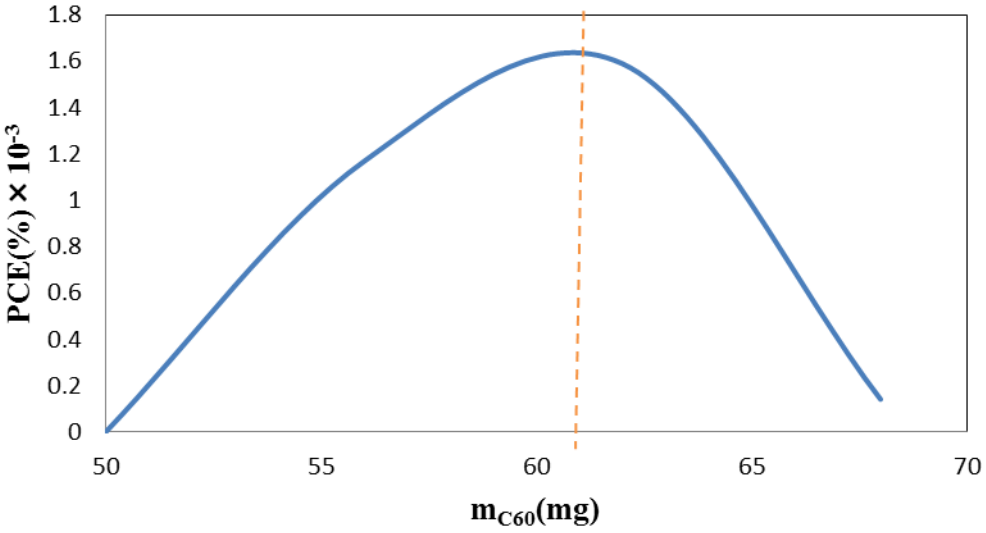

Figure 2-16 PCE changing with C60 weight

2.4 Conclusions

1. The first, PEDOT was synthesized by using chemical oxidative polymerization. Then C60-PEG/PEDOT gel, which form interpenetrate network structure, was prepared under low temperature(<70℃) organic solvent processed.

2. The C60-PEG/PEDOT gel was coated onto ITO glass by using spin-coater under the condition of 1000-2500 rpm to form the porous C60-PEG/PEDOT film. Then the film using this material was identified by SEM, FT-IR, XRD, UV response and UV-Vis absorption spectra measurement. The results showed that PEDOT was synthesized inside of C60-PEG gel, and that the C60-PEG/PEDOT gel has an amorphous structure on contrary to C60-PEG crystalline structures. The bandgap of C60-PEG/PEDOT material is smaller than C60-PEG materials, that is, C60-PEG/PEDOT material is stronger absorption of UV light than C60-PEG material.
3. Then we fabricated the polymer solar cells device using this composite

material, and it was confirmed the composite film showed UV response and power conversion efficiency by irradiating with UV or simulated sunlight. The results showed that UV response of C60-PEG/PEDOT device was much higher than C60-PEG device. It was considered that UV response was improved by synthesizing PEDOT into C60-PEG gel to form new interpenetrate network structure.

4. PCE of C60-PEG/PEDOT device was about 1.2×10-3 %. Fabricated bulk heterojuction polymer solar cells device by using C60-PEG/PEDOT film, the Jsc is more 10 times higher than C60-PEG/Pc device. Improved the PCE by changing the molar ratio of C60 and PEG, the result showed the best PCE is $1.6x10^{-3}$, when molar ratio of C60 to PEG has been optimized to approximately 1:4.

References

1. Martin, N., Sanchez, L., Illescas, B. & Perez, I. C60-based electroactive organofullerenes. Chem. Rev. 98, 2527−2547 (1998).
2. Taherpour, A.A. Quantitative structural relationship and theoretical study of electrochemical properties of C_{60}@[SWCN(5, 5)-Armchair-CnH20] Complexes .
   Chem.Phys.Lett.469, 135−139(2009).
3. Wu, J. W., Alemany, L.B., Li, W.L., Petrie, L., Welker, C. & Frotner, J.D. Reduction of hydroxylated fullerene (fullerol) in water by zinc: reaction and hemiketal product characterization. Environ.Sci.Technol.48,7384−7392(2014).
4. Guldi, D.M. & Prato, M. Excited-state properties of C_{60} fullerene derivatives.Acc.Chem.Res.33,695−703(2000).
5. Bendikov, M. & Wudi, F. Tetrathiafulvalenes, oligoacenenes, and their buckminsterfullerene derivatives: the brick and mortar of organic electronics.Chem.Rev.104,4891−4945(2004).
6. Allen, N. S., Zeynalov, E.B., Taylor, K. & Birkett, P. Antioxidant capacity of novel amine derivatives of buckminsterfullerene: Determination of inhibition rate constants in a model oxidation system. Polym. Degrad. Stabil.94, 1932−1940 (2009).
7. Zakharian, T. Y., Seryshev, A., Sitharaman, B., Gilbert, B.E., Knight, V. & Wilson, L.J. A fullerene-paclitaxel chemotherapeutic: synthesis, characterization, and study of biological activity in tissue culture. J.Am.Soc.127,12508−12509(2005).
8. Sudeep, P. K., Ipe, B.L., Thomas, K.G. & George, M.V. Fullerene-functionalized gold nanoparticles. a self-assembled photoactive antenna-metal nanocore assembly. Nano Lett. 2,29−35(2002).
9. Wrobel, D. & Graja, A. Photoinduced electron transfer processes in

fullerene–organic chromophore systems. Coord. Chem. Rev. 255, 2555 −2577(2011).

10. Magnel, G.-I., Peuntinger, K., Kahnt, A., Krausmann, J., Vazquez, P., David, G-R., Guldi, D. M. & Torros, T. Supramolecular assembly of multicomponent photoactive systems via cooperatively coupled equilibria. J.Am.Chem.Soc.135,19311−19318 (2013).
11. Hoppe, H., Niggemann, M., Winder, C., Krant, J., Hiesgen, R., Hinsch, A., Meissner, D. & Sariciftci, N.S. Nanoscale morphology of conjugated polymer/fullerene-based bulk-heterojunction solar cells. Adv.Funct.Mater.14,1005−1011(2004).
12. Brabec, C.J., Saeiciftci, N.S. & Hummelen, J.C. Plastic solar cells. Adv. Funct. Mater.11,15−26(2001).
13. Blach, A.L., Costa, D.A., Fawcett, W.R. & Winkler, K. Electronic communication in fullerene dimers. electrochemical and electron paramagnetic resonance study of the reduction of $C_{120}O$. J.Phys.Chem.100, 4823−4827(1996).
14. Jensen, A.W., Wilson, S.R. & Schuster, D.I. Biological applications of fullerenes. Biologan.Med.Chem.4, 767− 779(2006).
15. Fletcher, J.S., Lockyer, N.P. & Vickerman,J.C. C_{60}, buckminsterfullerene: its impact on biological ToF-SIMS analysis. Surf.Interface.Anal.38, 1393−1400(2006).
16. Bosi,s., Ros, T. D. Spalluto, G. & Prato, M. Fullerene derivatives: an attractive tool for biological applications. Eur.J.Med.Chem.38,913−923(2003).
17. Walker, B., Tamayo, A. B., Dang, X.-D., Zalar, P., Seo, J. H., Garcia, A.,Tantiwiwat, M. & Nguyen, T.-Q. Nanoscale phase separation and high photovoltaic efficiency in solution-processed, small-molecule bulk heterojunction solar cells. Adv. Funct. Mater.19, 3063−3069(2009).
18. Spanggaard, H. & Krebs, F. C. A brief history of the development of organic and polymeric photovoltaics. Sol. Energ. Mat. Sol. C. 83,

125−146(2004).

19. Wang, C., Guo, Z.-X., Fu, S., Wu, W. & Zhu, D. Polymers containing fullerene or carbon nanotube structures. Prog. Polym. Sci. 29, 1079−1141(2004).
20. Blouin, N., Michaud, A. & Leclerc, M. A low-bandgap poly(2,7-Carbazole) derivative for use in high-performance solar cells. Adv. Mater. 19, 2295−2300(2007).
21. Marcus, Y., Simth, A.L., Korobov, M. V., Mirakyan, A.L., Avramenko, N.V. & Stukalin, E. B. Solibility of C_{60} fullerene. J. Phys. Chem. B. 105, 2499−2506(2001).
22. Okamura, H., Ide, N., Minoda, M., Komatsu, K. & Fukuda, T. Solubility and micellization behavior of C_{60} fullerenes with two well-defined polymer arms. Macromolecules.31, 1859−1865(1998).
23. Giacalone, F. & Martin, N. Fullerene polymer: synthesis and properties. Chem.Rev.106, 5136−5190(2006).
24. Ederle, Y. & Mathis, C. Grafting of Anionic Polymers onto C60 in polar and nonpolar solvents. Macromolecules.30, 2546−2555(1997).
25. Moule, A. & Meerholz, K. Controlling morphology in polymer–fullerene mixtures. Adv. Mater.20,240−245 (2008).
26. Yu, G., Gao, J., Hummelen, J.C., Wudl, F. & Heeger, A.J. Polymer photovoltaic cells: enhanced efficiencies via a network of internal donor-acceptor heterojunctions. Science. 270,1789−1791(1995).
27. Theobald,J.A., Oxtoby, N.S., Phillips, M.A., Champness, N.R. & Beton, P.H. Controlling molecular deposition and layer structure with supramolecular surface assemblies. Nature. 424, 1029−1031(2003).
28. Ma, W., Gopinathan, A. & Heeger A.J. Nanostructure of the interpenetrating networks in poly(3-hexylthiophene)/fullerene bulk heterojunction materials: implications for charge transport. Adv. Mater.19,3656−3659(2007).
29. Wakai, H., Momoi, T., Shinno, T., Yamauchi, T. & Tsubokawa, N. A

novel polymer-grafted C_{60} fullerene having both hydrophilic and hydrophobic chains. Mater. Chem.Phys.118,142−147(2009).

30. Wakai, H., Shinno, T., Yamauchi, T. & Tsubokawa, N. Grafting of poly(ethylene oxide) onto C_{60} fullerene using macroazo initiators. Polymer.48,1972−1980(2007).
31. Wakai, H., Momoi, T., Yamauchi, T. & Tsubokawa, N. A simple preparation of C_{60}-poly(ethylene glycol) gel and its properties. Polym.J.41,40−45(2009).

Chapter 3

Preparation of microrods structure C60- PEG and PEDOT composite film by a novel template method and application for organic photovoltaic devices

Abstract

Microrods structure film with many nanoscale layered sheets around the rod, that mimicked unique functionalities of antireflective moth eyes, are fabricated by a novel template method using C60-PEG/PEDOT composite gel under low-temperature by organic-solvents processed. Its optical, electrical and photoelectric properties are evaluated. The UV-Vis absorption spectra shows a redshift of the microrods structure, and cyclic voltammetry(CV) measurement result shows the bandgap of the active layer with the microrods structure is 2.57eV, which is narrow than 2.65eV of the active layer with flat structure. Power conversion efficiencies(PCE) of the device of the active layer with microrods structure and the device added a PEDOT:PSS layer between ITO glass and the microrods structure active layer are more higher than the device of flat structure, respectively.

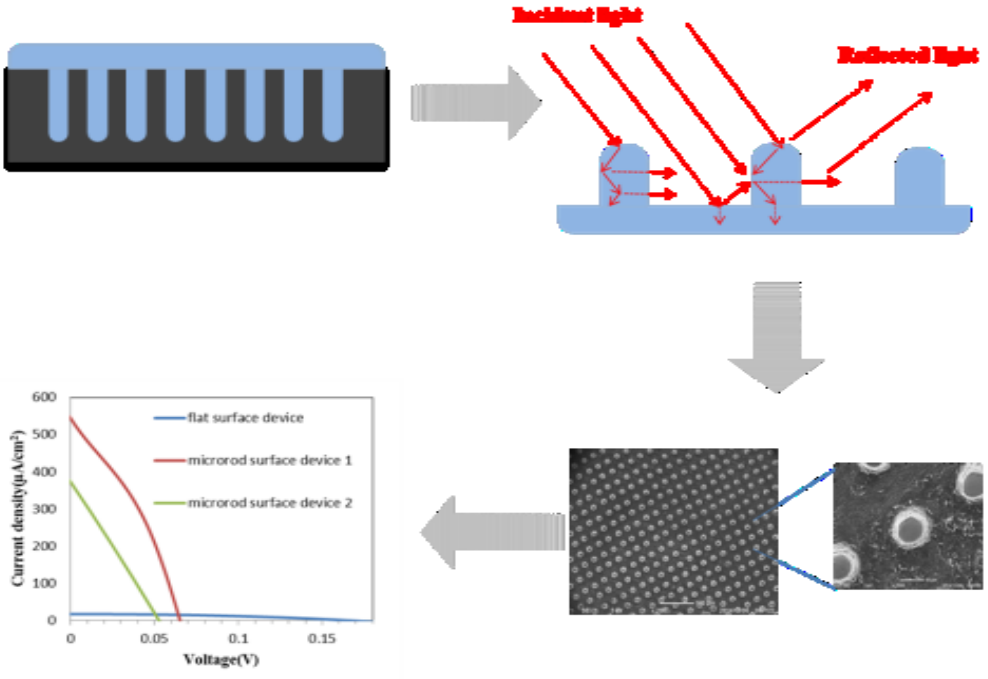

Figure 3-1 Schematic representation of this chapter

3.1 Introduction

C60 fullerene had attracted much attention during it was discovered in 1985,[1-3] because of its remarkable properties, such as the interaction with light,[4-6] accepting and releasing electrons ability,[7,8] trapping free radical,[9] and photo-activity.[10] Those properties were related to photochemical and photo-induced charge transfer properties of C60 fullerene.[11] For example, solar energy conversion and storage.[12] However, the poor solubility of C_{60} fullerene in most solvent hampered its applications in the most fields. [13] Hence various types of useful methods had been reported. [14, 15] In particular, a grafting of polymer chains onto C_{60} fullerene had aroused interest,[16] because not only this C60 fullerene derivative can improve the solubility of C_{60} fullerene, but can also form the network structure materials, which was able to enhance some properties, such as photoelectrical character using for solar cells.[17-20]

In the natural world, there are many inspirations for scientists to mimic the unique functionalities of biological systems for practical applications, for example, antireflection[21-25] and anti-glaring[26] of moth eye microstructure and lotus effect or self-cleaning effect of lotus leaves microstructure(Figure 3-2). It was estimated that these special properties were able to use for solar cells devices, such as collecting sunlight to improve the PCE.

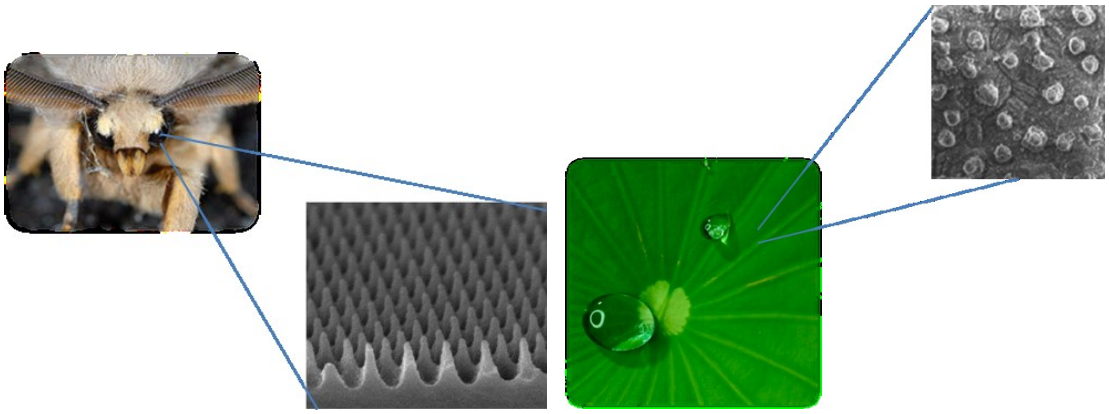

Figure 3-2 Moth eye and lotus effect microstructure.

In our previous work, we had reported that poly(ethylene glycol)(PEG) radicals were successfully trapped on C_{60} fullerene surface to formed C_{60}-PEG gel,[27-29] which was able to composite with poly(3,4-ethylenedioxythiophene)(PEDOT) by chemical oxidative polymerization. Then we fabricated the polymer solar cells (PSCs) device using this composite material, and investigated the UV response of C60-PEG/PEDOT device was much higher than C60-PEG device. It was estimated that UV response was improved by synthesizing PEDOT into C60-PEG gel to form new interpenetrate network structure. PCE of C60-PEG/PEDOT device was about 1.2×10-3 %.[30] It was considered that the loss in PCE arises from the decreased Jsc, which could result from the light would be reflected on the film surface. For solving this problem, it was necessary for surface modification of active layer, and the optimization of film surface morphology are more and more important in this research field.

In this chaper, mimicking the moth eyes, we signed a novel, cost-effective template method to prepare the microrods structure film with many nanoscale layered sheets on the surface using PEG/PEDOT materials.[31, 32] The film was identified by scanning electron microscope (SEM), Fourier transform infrared (FT-IR) spectroscopy, UV-Vis absorption spectra and CV measurement. Then, we fabricated M1(Supporting Information) and M2(Supporting Information) using those film as the active layer, and compared with the photoelectrical property of F1(Supporting Information), and discuss the effect factor of the short circuit current density(J_{sc}), the open circuit voltage (V_{oc}), and fill factor(FF) of the device.

3.2 Experimental

3.2.1 Materials and reagents

The C60 fullerene used was "nanom purple N60-ST", obtained from Frontier Carbon Corporation Co., Ltd., which was used without further purification. The purity was greater than 96% and average particle size was 30-70μm. C60 fullerene was dried in vacuum at 50 °C before use.

Macro azo-initiator, (Azo-PEG)n, was commercially obtained from Wako Pure Chemical Industries, Ltd, Japan (commercial name of the (Azo-PEG)n was VPE-0201). The molecular weight of PEG unit was 2.0 x 10^3 and it contains several azo groups, which can form polymer radical.

3,4-ethylendioxythiophene (EDOT) obtained from Sigma Aldrich Co., LLC., which was used without further purification.

3.2.2 Reaction of C_{60} fullerene and PEG

Scheme 3-1 shows the reaction of C_{60} fullerene and PEG. Detailed methods are shown in the Chapter 2 (Section 2.2.3).

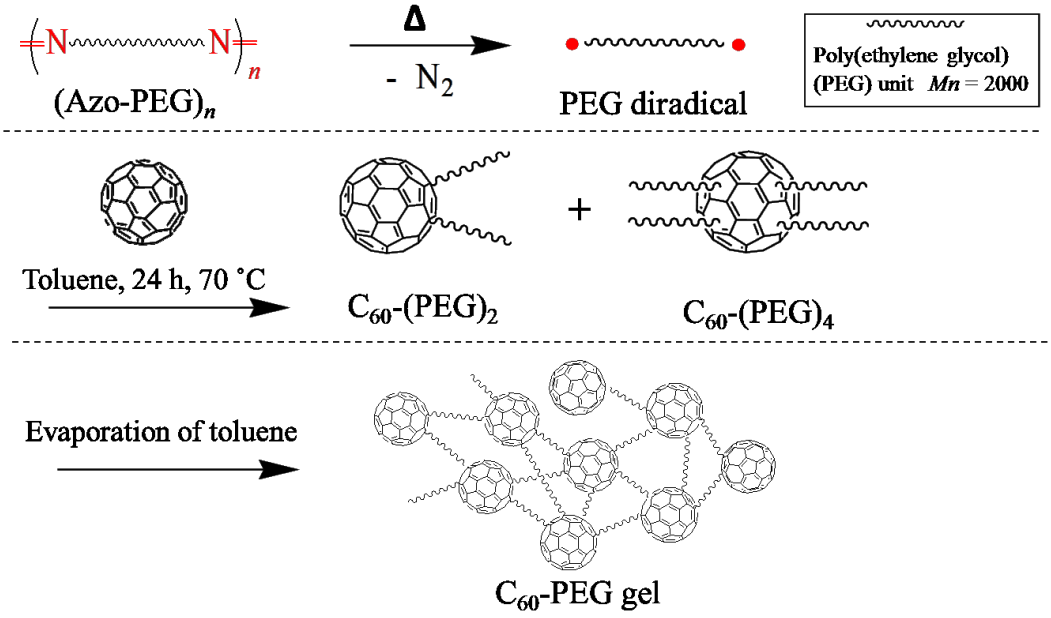

Scheme 3-1 Reaction of C_{60} fullerene and PEG

3.2.3 Preparation of C60-PEG/PEDOT gel

3.2.3.1 Synthesis PEDOT by chemical oxidative polymerization

PEDOT was synthesized by chemical oxidative polymerization. $FeCl_3$ was dissociated to Fe^{3+} and 3Cl- in EDOT/$FeCl_3$ toluene solution. Once EDOT and Fe^{3+} contacted, the polymerization of EDOT was initiated by moving an electron from EDOT to Fe^{3+}. EDOT works as an active center and was added to another EDOT molecule. This process was repeated many times and PEDOT was obtained , shown in Scheme 3-2.

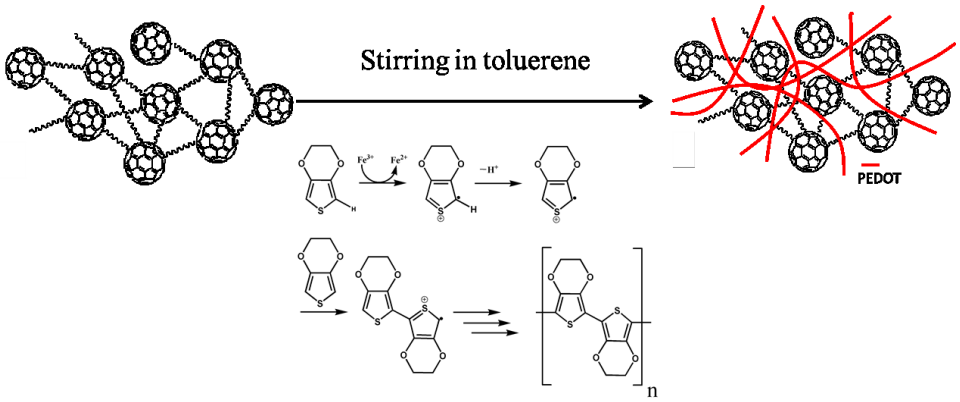

Scheme 3-2 Synthesis of PEDOT by chemical oxidative polymerization

3.2.3.2 The preparation process of C60-PEG/PEDOT gel

Before C60-PEG sol was prepared, $FeCl_3$ was used as an oxidative agent and EDOT/FeCl3 solution was prepared by mixing EDOT and $FeCl_3$ in toluene. Then EDOT/FeCl3 solution was added into C60-PEG sol, and dropped this sol onto ITO glass, after drying at 60°C for three days, C60-PEG/PEDOT gel was prepared.

3.2.4 Fabrication process of polymer solar cells device

3.2.4.1 Fabrication microrods structure film

Schematic representation of fabrication microrods structure film was shown in Figure 3-3, Using porous template, dropping C60-PEG/PEDOT gel onto this template, after drying it, we got the microrods structure film.

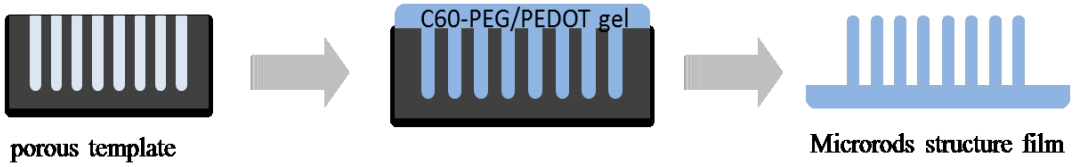

Figure 3-3 Schematic representation of fabrication microrods structure film

3.2.4.2 Fabrication process of PSCs device with microrods structure active layer

C_{60}-PEG/PEDOT gel was evaporated by rotary evaporation under the condition of 40 Degrees Celsius, 50mmHg (millimeter mercury), then this gel was coated onto ITO glass using spin-coater at 1000-2500rpm (revolutions per minute). After 30s, active layer film was ready. Then, this film was dried at 60 degrees Celsius for 72 hours. Then used template method to mimic the moth eye structure, the microrods film by using porous template was obtained(Figure 3-4).

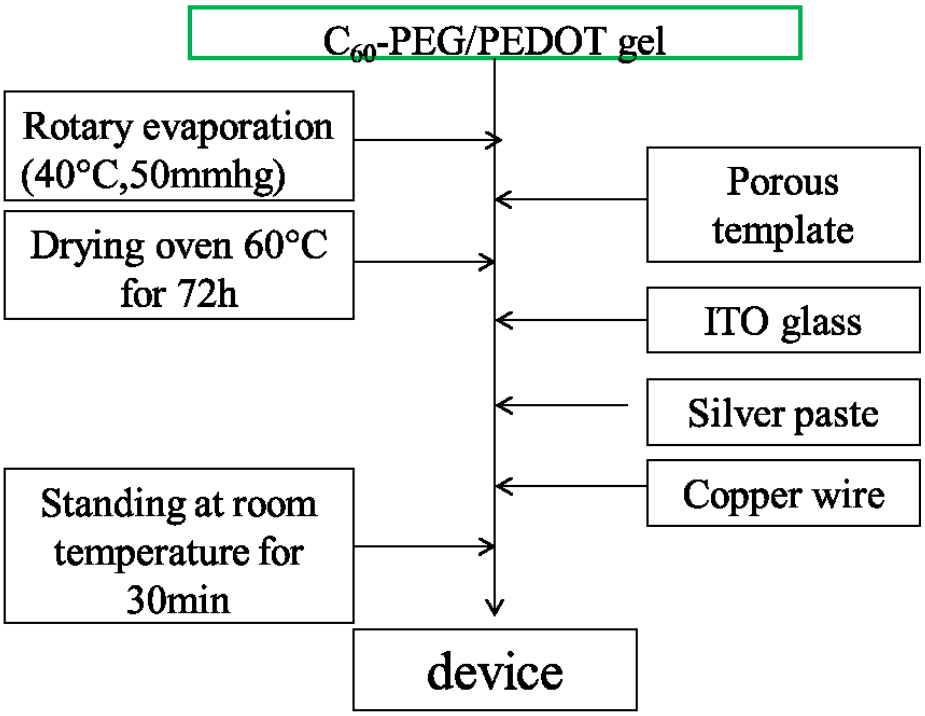

Figure 3-4 Fabrication process of photovoltaic device of polymer solar cells

3.2.5 Measurement

For measuring the characteristic of the composited gel, C60-PEG/PEDOT gel was dried to make a C60-PEG/PEDOT film.

SEM was recorded with a LEOL Ltd. JSM-6510.

Infrared spectra were recorded on a FT-IR spectrophotometer, Shimazu Manufacturing Co., Ltd. FTIR-8400S.

UV–vis absorption spectra were recorded on a UV-1800(Shimadzu Corp.).

Cyclic voltammetry was done on a HZ5000 Potentiostat /Galvanostat (HSV-100, HOKUTO DENKO Corp.) with platinum electrodes at a scan rate of 50 mV s^{-1} against an Ag/AgCl reference electrode at room temperature under an atmosphere of nitrogen with a scanning rate of 20 mV/s.

Porous template with 8 μm pitch on the surface by photolithography was received from Kyoto University (made by Electronics and Materials Corporation), including three materials template, the Copper, Aluminium and crystalline silicon materials.

Photocurrent was measured when voltage applied from - 1.0 V to 1.0 V by irradiating a solar simulator (HAL-C100, 100 W compact xenon light source, ASAHI SPECTRA) with AM1.5G spectra at 100 $mWcm^{-2}$ at room temperature.

3.2.6 Power conversion efficiency

Power conversion efficiency (PCE) of the device of the active layer with C_{60}-PEG/PEDOT flat structure and the device of the active layer with C_{60}-PEG/PEDOT microrods structure was investigated. The devices were fabricated using C_{60}-PEG/PEDOT gel which was connected with copper line by Ag paste. Photocurrent was measured when voltage applied from -

1.0 V to 1.0 V by irradiating a solar simulator (HAL-C100, 100 W compact xenon light source, ASAHI SPECTRA) with AM1.5G spectra at 100 mW cm^{-2} at room temperature. Dark current was measured under the same conditions without simulated sun light.

3.3 Results and Discussion

3.3.1 Fabrication of microrods structure film

PEDOT was synthesized inside of C60-PEG gel by dropping FeCl3/EDOT solution, C60-PEG gel and PEDOT formed C60-PEG/PEDOT gel, a composite material which has network structure. All of the synthesis processes were in the conditions of organic-solvent under the low temperature. Then dropping or coating this C60-PEG/PEDOT composite material onto porous template. After drying it, the microrods structure film using C60-PEG/PEDOT material was obtained (shown in Figure 3-7).

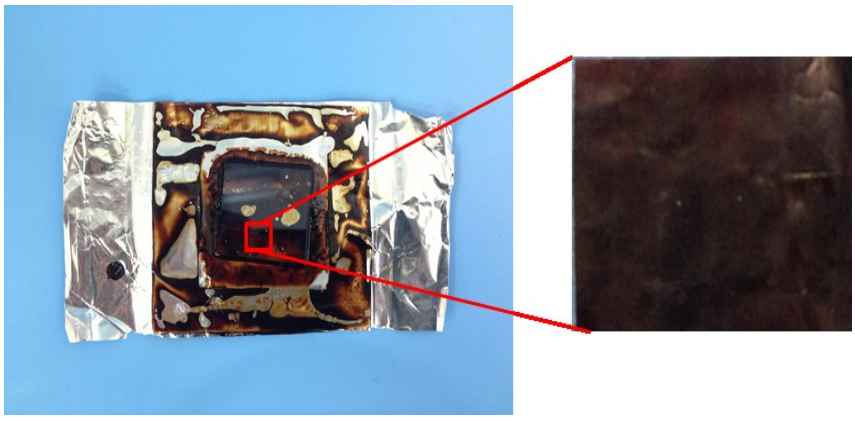

Figure 3-5 Photographs of Al porous template and C60-PEG/PEDOT composite material microrods film

3.3.2 The morphology of microrods film and template surface

The surface morphologies of C60-PEG/PEDOT film and template were observed utilizing SEM, the top SEM image of the template surface was shown in Figure 3-7, and the top SEM images of the microrods structure film was shown in Figure 3-8. The microrods structure was confirmed from

the surface of C60-PEG/PEDOT film. There were lots of uniform microrods onto film surface, and the diameter of the rod became lager from top to bottom. In this image, there are many nanoscale layered sheets around the rod (shown in Figure 3-9), just like moth eye structure, which would be a great effect on the light absorption.

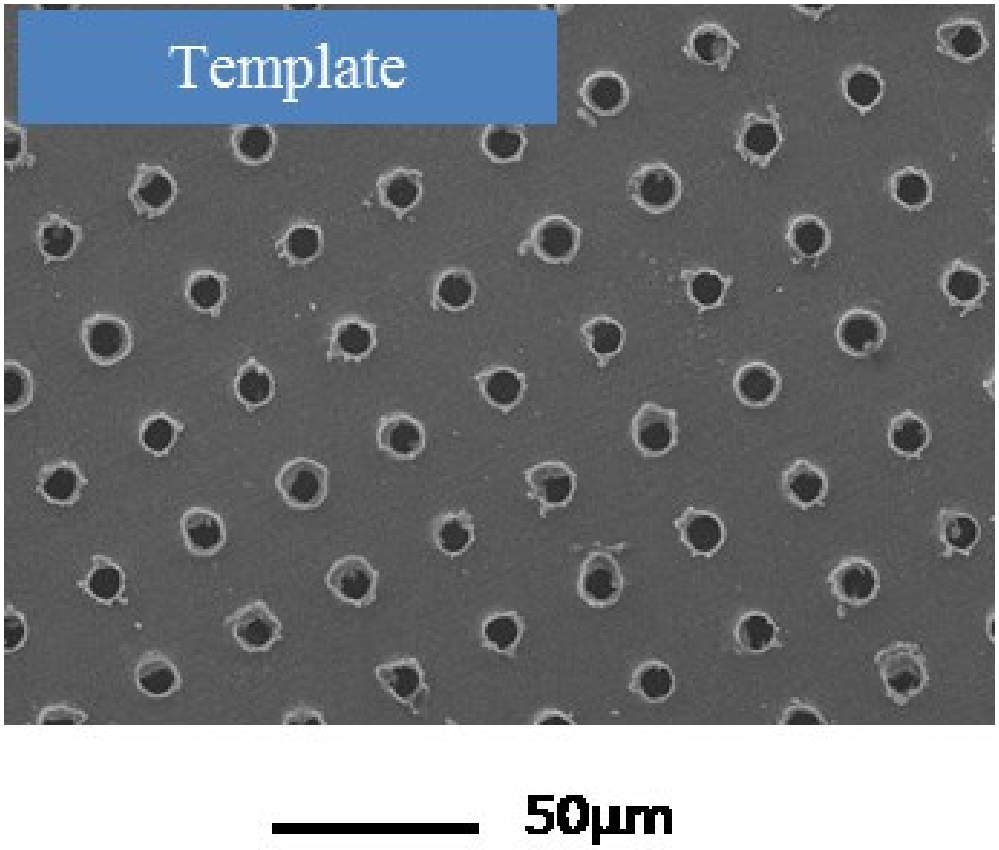

Figure 3-6 SEM image of Al porous template

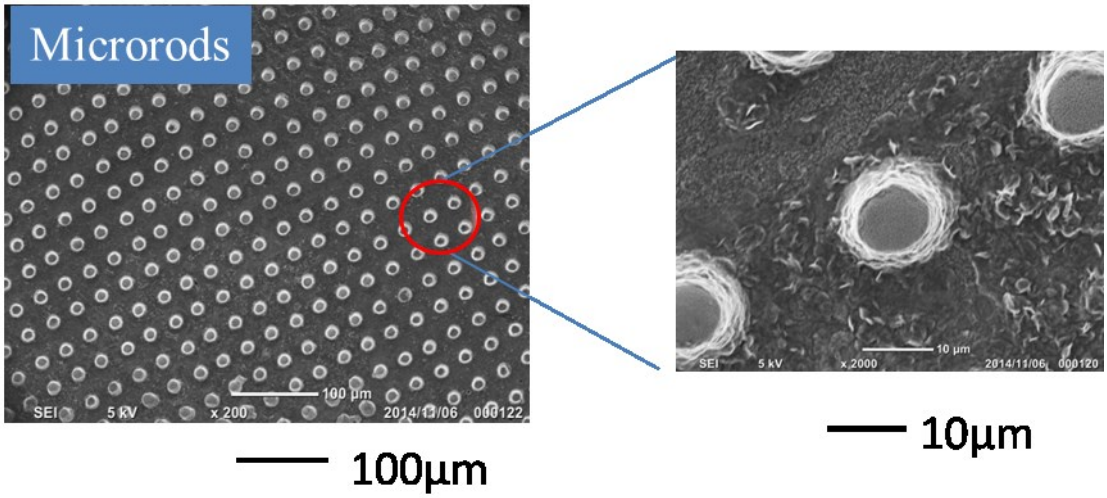

Figure 3-7 SEM imageS of microrods structure film

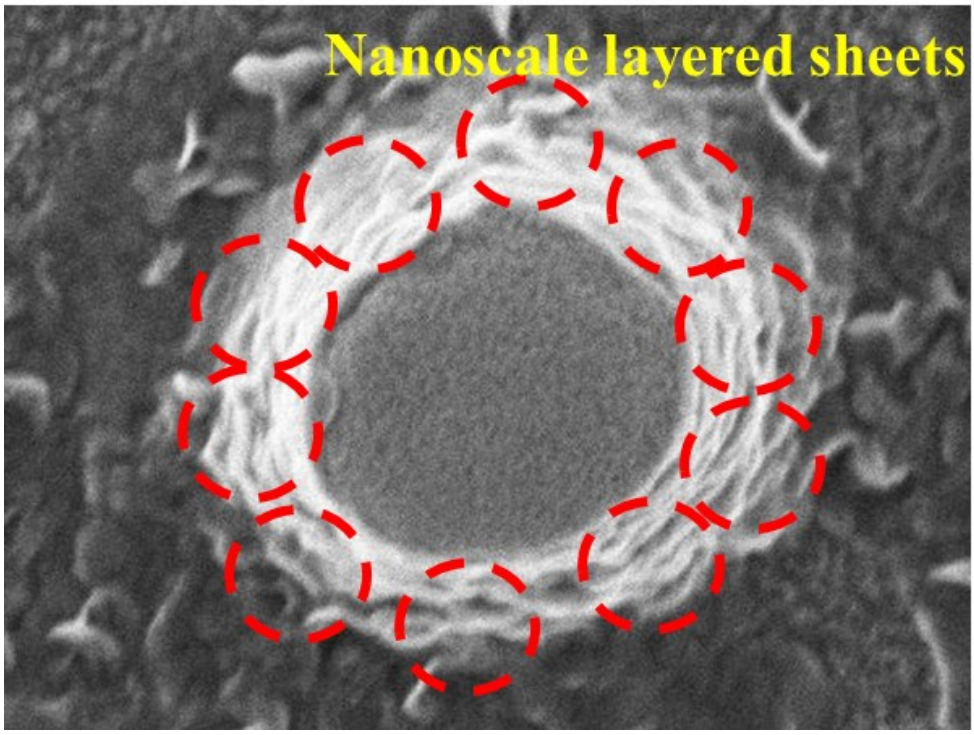

Figure 3-8 SEM image of lots of nanoscale layered sheets around the rod

3.3.3 FT-IR spectrum

Figure 3-10 showed FT-IR spectra of PEDOT and C60-PEG/PEDOT film with microrods structure. In the spectrum of C60-PEG/PEDOT, there

were characteristic absorptions of methylene at 2925 cm^{-1} and enoxy at 1105 cm^{-1}, which were from C60-PEG material; and there are characteristic absorptions of thiophene at 1520 cm^{-1}, which were from PEDOT.

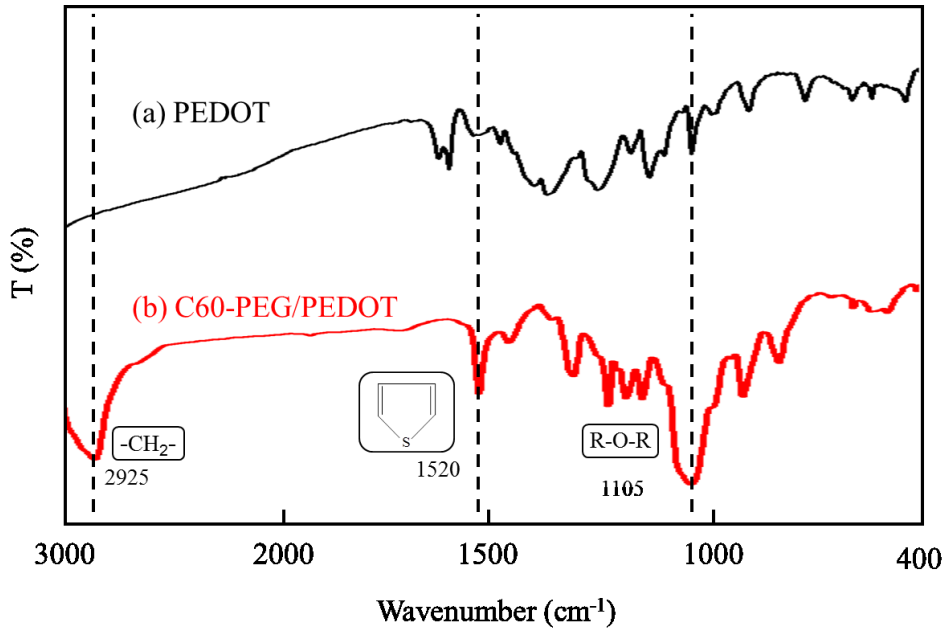

Figure 3-9 FT-IR spectra of (a) PEDOT (b) drying C60-PEG/PEDOT microrods structure film

3.3.4 UV response of C_{60}-PEG/PDOT film

UV-Vis absorption spectra of the flat structure film and the microrods structure film show in figure 3-11. This two thin films prepared by the same material, the difference point was only on the film surface structure. In Figure 3-11, the flat structure film and the microrods structure film show an absorption maximum(λ_{max}) wavelength at 335nm and 340nm, respectively, Which are from the π-π^* transition of the conjugated system.[33, 34] The peak of the microrods structure film shows a significantly redshift from the peak of the flat structure film. It is estimated that such red shift was attributed to bandgap narrowing, so we calculated the bandgap of the flat structure film and the microrods structure film (shown in Table 3-1). The absorption edges of the flat structure film and the microrods structure film are at 470nm and 482nm, respectively. The optical bandgap ($E_{g,opt}$) for the flat structure film

and the microrods structure film are 2.64eV and 2.57eV, respectively. The result shows that the bandgap of the microrods structure film is smaller than the flat structure film, that is, the microrods structure film is stronger absorption of UV light than the flat structure film.

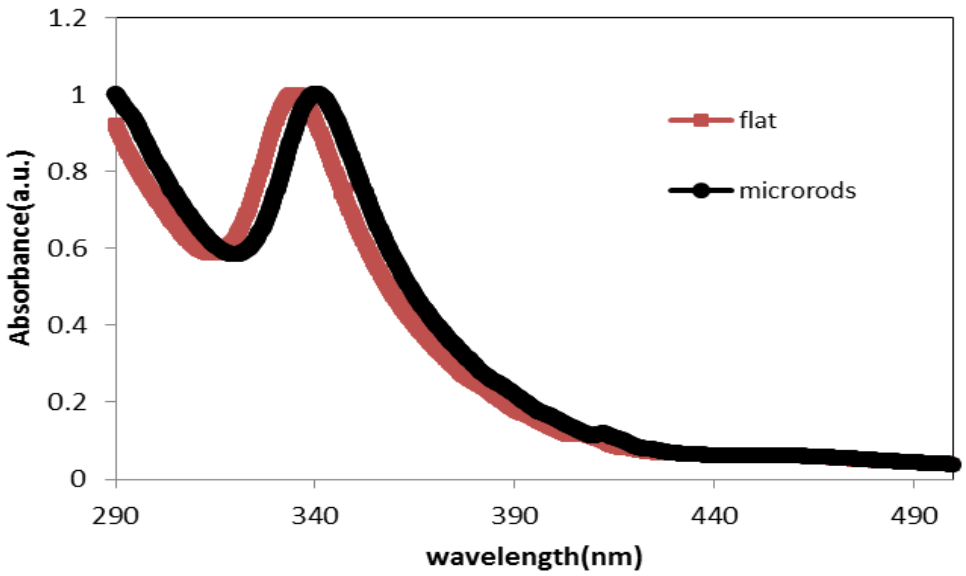

Figure 3-10 UV-Vis absorption spectra of the flat structure film and the microrods structure film

3.3.5 Cyclic voltammetry of C60-PEG/PDOT films

The oxidation onset of the flat structure film and the microrods structure film measured by cyclic voltammetry (CV) were 0.53V and 0.48V, respectively. The CV curves were shown in Figure 3-12(a) and (b). According to the equation $E_{HOMO}= -(E_{ox}+4.71)(eV)$,[35-37] highest occupied molecular orbital(HOMO) energy level of the flat structure film and the microrods structure film were calculated to be -5.14eV and-5.09eV, respectively. The lowest unoccupied molecular orbital (LUMO) energy of the flat structure film and the microrods structure film were calculated to be -2.49 eV and -2.52 eV by using the equation $E_{LUMO}=E_{HOMO}+E_{g,opt}$. The data were summarized in Table 3-1. It was obvious that the HOMO energy of this two films were both deeper than the work function of ITO glass, and

bandgap of the microrods structure film was 0.08eV narrow than the flat structure film, which was just as previously discussion at UV-Vis absorption spectra.

Table 3-1 Physical, electronic, and optical properties of microrod structure C60-PEG/PEDOT and flat structure C60-PEG/PEDOT

Material	λ_{max}	$E_{g,OPT}$ [a)]	HOMO	LUMO
	[nm]	[eV]	[eV]	[eV]
F1	335	2.65	-5.14	-2.49
M1	340	2.57	-5.09	-2.52

[a)] calculated from the absorption band edge of the film, $E_{g,OPT}=1240/\lambda_{edge}$

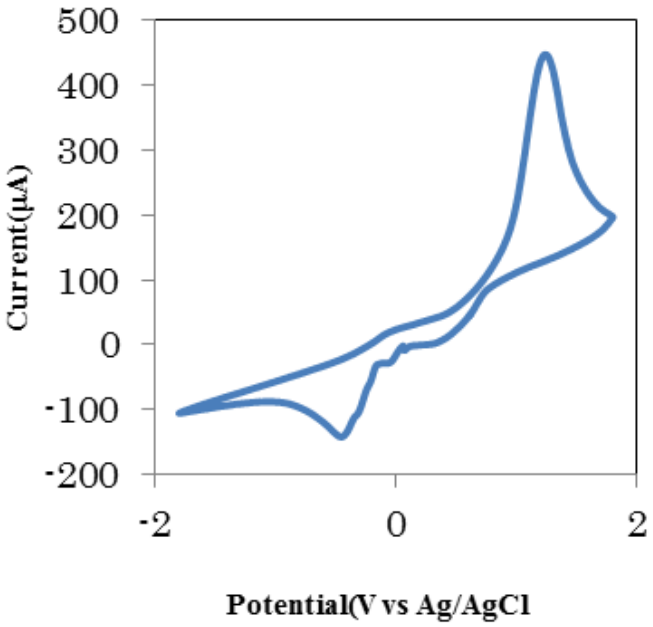

(a)

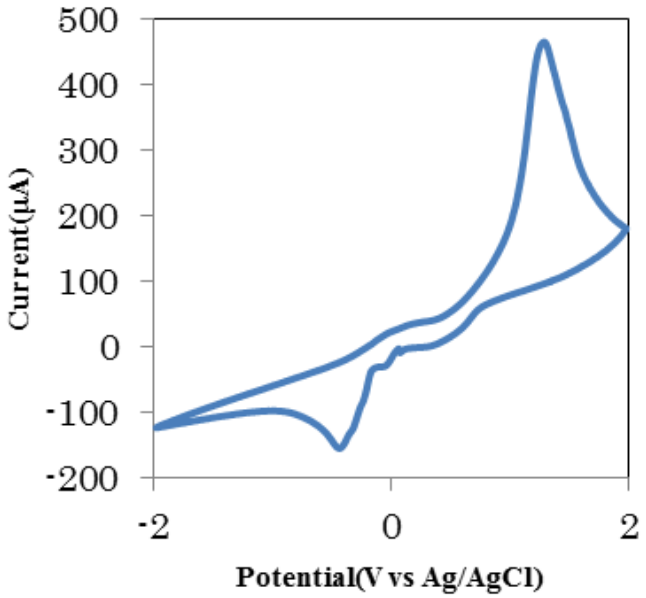

(b)

Figure 3-11 Cyclic Voltammogram of the film with (a) the flat structure film (b) the microrods structure film

3.3.6 Photovoltaic property

PSCs devices were fabricated using C60-PEG/PEDOT films with microrods structure and without mocrorods structure as active layer. A PCE of $9.73x10^{-3}$% with Voc of 0.05V, Jsc of 54.4μA cm^{-2} ,and FF of 0.33 was obtained from the device added a PEDOT:PSS layer between ITO glass and the microrods structure active layer, and PCE of $5.43x10^{-3}$ % with Voc of 0.05V, Jsc of 37.3μA cm^{-2} ,and FF of 0.28 was obtained from the device of the active layer with the microrods structure, respectively, measured when voltage applied from - 1.0 V to 1.0 V by irradiating a solar simulator (HAL-C100, 100 W compact xenon light source, ASAHI SPECTRA) with AM1.5G spectra at 100 $mWcm^{-2}$ at room temperature. The current density-voltage (J-V) characteristics of the BHJ PSCs were shown in Figure 3-13. Parameters of the device of the active layer with flat

structure, the device of the active layer with the microrods structure and the device added a PEDOT: PSS layer between ITO glass and the microrods structure active layer fabricated under room temperature were shown in Table 3-2. Comparison with the PCE of the device of the active layer with flat structure, the device of the active layer with the microrods structure and the device added a PEDOT:PSS layer between ITO glass and the microrods structure active layer, the PCEs of those two devices were more higher than the device of the active layer with flat structure. It was suggested that after modifying the surface and adding the hole transporting layer(PEDOT:PSS),[38] Jsc was from 16.8μAcm^{-2} to 37.3μA cm^{-2}, 54.4μA cm^{-2},respectively, which shown remarkable increase of 2times and 3 times, respectively.

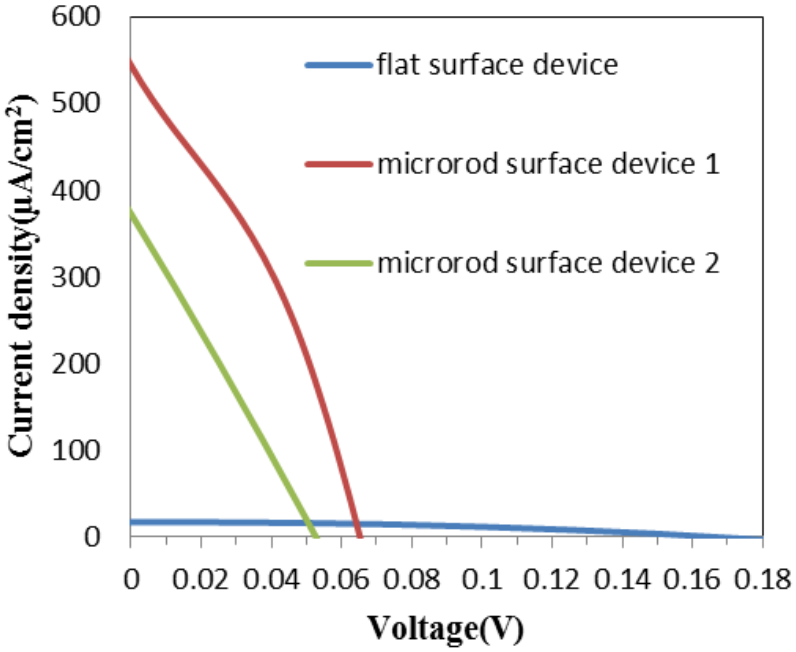

Figure 3-12 *J-V* characteristic of BHJ PSCs with flat structure and microrods structure C60-PEG/PEDOT-based devices fabricated from toluene under room temperature.

Table 3-2 Parameters of F1 (flat structure), M1 (microrods structure) and M2 (added a PEDOT:PSS layer between ITO glass and the microrods

structure active layer) C60-PEG/PEDOT-based devices fabricated from toluene under room temperature.

Surface Morphology	J_{sc} [μAcm^{-2}]	V_{oc} [V]	FF [%]	PCE [%]x10^{-3}
F1	16.8	0.16	42.26	1.20
M1	37.3	0.05	27.7	5.43
M2	54.4	0.05	33.0	9.73

3.3.7 The influence of J_{sc} by Surface modification of film

Figure 3-14 shown propagation of incident light through a microrods structure film. Surface modification would effect the short circuit current on two sides: the photo-induced charge carrier density and the charge carrier mobility in theory.[39]

$$\mathbf{Jsc = ne\mu E} \qquad (1)$$

Where n is the density of charge carriers; e is the elementary charge; μ is the mobility; E is the electric field

On one hand, the incident light would be scattered onto the surface of the microrods structure with many nanoscale layered sheet active layer, the reflected light would be weakened, so more light would be trapped into the active layer to improve the photo-induced charge carrier density (shown in Figure 3-14).

On the other hand, the microrods structure interface area would be more bigger, which afforded a better chance for the excitons to be separated when the separation occurs at the interface of the donor and acceptor (shown in Figure 3-15), because the hole and electrode would be easy to reach the surface of active layer, which was more effective on the rods surface. Thus the recombination ratio of charge carrier would be decreased remarkably, that is, the mobility of charge carriers would be increased in the active layer. After the density of charge carriers and the the mobility of charge carriers are improved, the J_{sc} will be improved, so the PCE will be improved, which is

shown in Table 2.

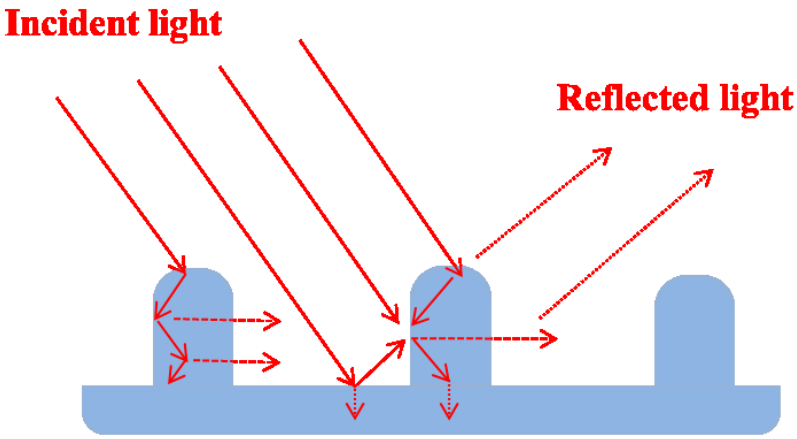

Figure 3-13 Propagation of incident light through a microrods structure film

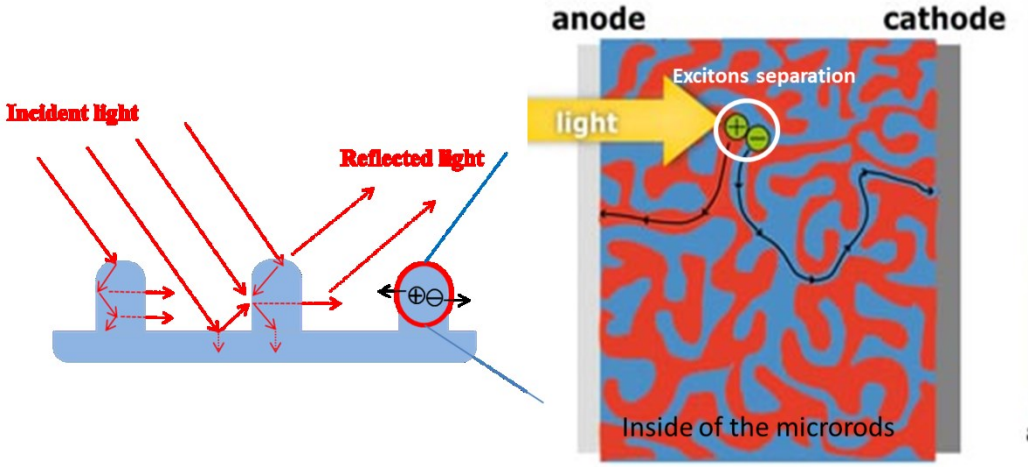

Figure 3-14 Graphical representation of excitons separation inside a micro rod

3.3.8 Comparison of photoelectrical properties

Figure 3-16 the photoelectrical properties of flat structure device and microrods structure device. The PCE shows a remarkable increase as the structure change, which is caused by Jsc increase.

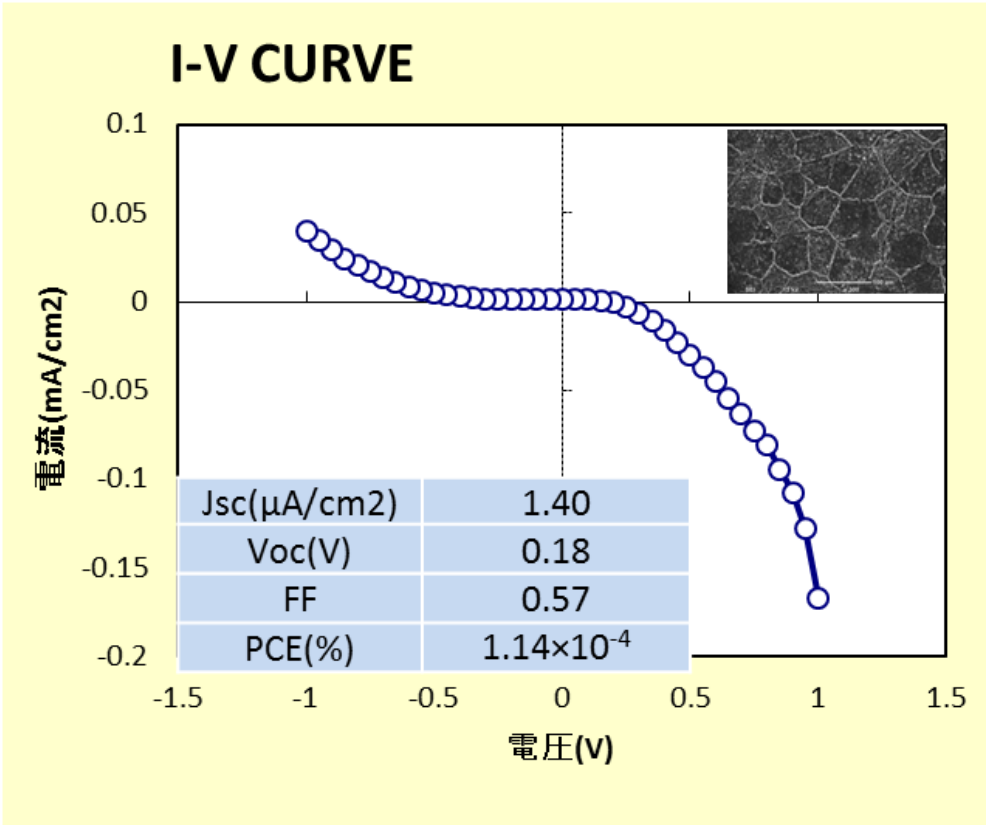

(a)

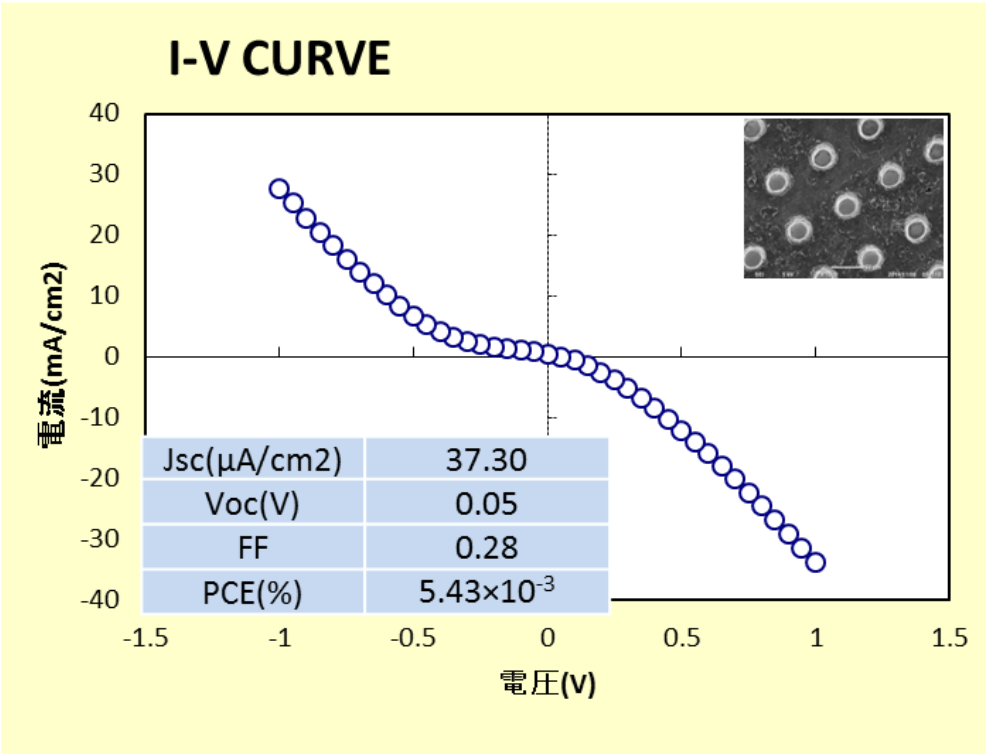

(b)

Figure 3-15 Photo current curves of (a) the flat surface device (b) the

microrods surface device.

The comparison of photoelectrical property of this two difference structure device shows in Table 3-3. Under the same condition, the microrods structure devices are remarkable improvement on the short circuit current, which is caused by surface modification. That is, the PCE was improved

Table 3-3 Photoelectrical properties of this two difference structure devices under 100 mW/cm2 AM1.5G of simulated solar illumination at room temperature

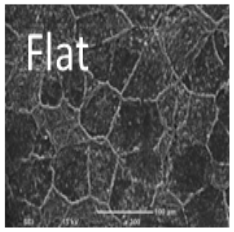

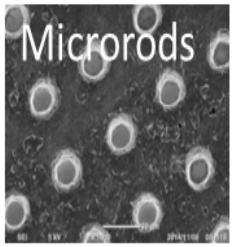

Material	J_{SC} (μA/cm²)	V_{OC} (V)	FF	PCE (%)
[b]C60-PEG/PEDOT	1.4	0.18	0.57	1.14×10^{-4}
[b]C60-PEG/PEDOT	16.8	0.17	0.42	1.16×10^{-3}
[b]C60-PEG/PEDOT	10.4	0.20	0.75	1.58×10^{-3}
[c]C60-PEG/PEDOT	21.4	0.03	0.18	1.26×10^{-3}
[c]C60-PEG/PEDOT	37.2	0.05	0.27	5.43×10^{-3}
[c]C60-PEG/PEDOT	54.4	0.05	0.33	9.73×10^{-3}

3.3.9 Other influence effector

Voc was linearly dependent on HOMO level of the donor and LUMO level of the acceptor.[39] In here, the donor was PEDOT, HOMO level of PEDOT was about -3.17eV.[40] Referring to the linear relation between the HOMO level of the conjugated polymer and the Voc.[41, 42] The Voc of the C60-PEG/PEDOT device would be 0.5V. However, in this three kinds of device, the most Voc was only 0.16V, the reason was estimated that the interfacial effects at the electrode and active layer interface changed the work function and influence the Voc. FF was determined by a balanced transport of electrons and holes,[43] the conductivity of the electrodes and active layer, and the contact resistance between interfacial and active layers.[44]

3.4 Conclusions

1. Mimicking the unique antireflection functionalities of moth eye microstructure, microrods structure film with lots of nanoscale layered sheet on the rod were fabricated by template method at room temperature.
2. The top SEM images shown the microrods structure surface morphology, UV-Vis absorption spectra shown a significantly red shift of microrods structure film, it was estimated that it would be attributed to bandgap narrowing along with the structure changing. Then CV measurement provided a reference that the bandgap of microrods structure film was 0.08eV narrow than the flat structure film.
3. From the results of UV-Vis absorption and CV measurement, it was demonstrated that the microrods structure film would increase the light absorption.
4. Fabricated bulk heterojuction polymer solar cell devices by using C60-PEG/PEDOT microrods material film, and measured the PCE, Which was more higher than the flat structure one
5. In particular, the Jsc had a remarkable increase revealed that the microrods structure not only was able to trap more light to improve the photoinduced chage carrier density, but can improve the mobility of charge carriers.

References

1. N. Martín, L. Sánchez, B. Illescas, I. Pérez, *Chem. Rev.* **1998**, *98*, 2527.
2. A. A. Taherpour, *Chem. Phys. Lett.* **2009**, *469*, 135.
3. J. Wu, L. B. Alemany, W. Li, L. Petrie, C. Welker, J. D. Fortner, *Environ. Sci. Technol.* **2014**, *48*, 7384.
4. D. Wróbel, A. Graja, Coordin Chem Rev 2011, 255, 2555.
5. M. Garcia-Iglesias, K. Peuntinger, A. Kahnt, J. Krausmann, P. Vazquez, D. Gonzalez-Rodriguez, D. M. Guldi, T. Torres, *J Am Chem Soc* **2013**, *135*, 19311.
6. H. Hoppe, M. Niggemann, C. Winder, J. Kraut, R. Hiesgen, A. Hinsch, D. Meissner, N. S. Sariciftci, *Adv. Funct. Mater.* **2004**, *14*, 1005.
7. D. M. Guldi, M. Prato, *Accounts Chem Res* **2000**, *33*, 695.
8. M. Bendikov, F. Wudl, D. F. Perepichka, *Chem. Rev.* **2004**, *104*, 4891.
9. N. S. Allen, E. B. Zeynalov, K. Taylor, P. Birkett, *Polym Degrad Stabil* **2009**, *94*, 1932.
10. T. Y. Zakharian, A. Seryshev, B. Sitharaman, B. E. Gilbert, V. Knight, L. J. Wilson, *J. Am. Chem. Soc.* **2005**, *127*, 12508.
11. N. S. S. By Christoph J. Brabec, Jan C. Hummelen, *Adv. Funct. Mater.* **2001**, *11*, 15.
12. M. Rincon, H. Hu, J. Campos, J. Ruiz-Garcia, *J Phys Chem B* **2003**, *107*, 4111.
13. Y. Marcus, A. L. Smith, M. Korobov, A. Mirakyan, N. Avramenko, E. Stukalin, *J Phys Chem B* **2001**, *105*, 2499.
14. H. Okamura, N. Ide, M. Minoda, K. Komatsu, T. Fukuda, *Macromolecules* **1998**, *31*, 1859.
15. F. Giacalone, N. Martin, *Chem. Rev.* **2006**, *106*, 5136.
16. Y. Ederle, C. Mathis, *Macromolecules* **1997**, *30*, 2546.
17. A. J. Moulé, K. Meerholz, *Adv. Mater.* **2008**, *20*, 240.

18. G. Yu, J. Gao, J. C. Hummelen, F. Wudl, A. J. Heeger, *Science* **1995**, *270*, 1789.
19. J. A. Theobald, N. S. Oxtoby, M. A. Phillips, N. R. Champness, P. H. Beton, *Nature* **2003**, *424*, 1029.
20. W. Ma, A. Gopinathan, A. J. Heeger, *Adv. Mater.* **2007**, *19*, 3656.
21. J. Cai, L. Qi, *Mater. Horiz.* **2015**, *2*, 37.
22. P. Ke, X.-N. Jiao, X.-H. Ge, W.-M. Xiao, B. Yu, *RSC Adv.* **2014**, *4*, 39704.
23. S. Thiyagu, B. P. Devi, Z. Pei, *Nano Res* **2011**, *4*, 1136.
24. B. Parida, S. Iniyan, R. Goic, *Renew Sust Energ Rev* **2011**, *15*, 1625.
25. C.-H. Sun, P. Jiang, B. Jiang, *Appl Phys Lett* **2008**, *92*, 061112.
26. J. Zhang, S. Shen, X. X. Dong, L. S. Chen, *Opt. Express* **2014**, *22*, 1842.
27. H. Wakai, T. Shinno, T. Yamauchi, N. Tsubokawa, *Polymer* **2007**, *48*, 1972.
28. H. Wakai, T. Momoi, T. Shinno, T. Yamaudhi, N. Tsubokawa, *Mater. Chem. Phys.* **2009**, *118*, 142.
29. H. Wakai, T. Momoi, T. Yamauchi, N. Tsubokawa, *Polym J* **2009**, *41*, 40.
30. H. Zhang, M. Ichinose, H. Takahashi, S. Tamesue , T. Mitsumata, M. Yagi, N. Tsubokawa, T. Yamauchi, *Polym J* **2015**, *accepted*.
31. Y. Liu, J. Goebl, Y. Yin, *Chem Soc Rev* **2013**, *42*, 2610.
32. J. Jang, M. Chang, H. Yoon, *Adv. Mater.* **2005**, *17*, 1616.
33. D. A. Egbe, S. Turk, S. Rathgeber, F. Kuhnlenz, R. Jadhav, A. Wild, E. Birckner, G. Adam, A. Pivrikas, V. Cimrova, *Macromolecules* **2010**, *43*, 1261.
34. S. Günes, A. Wild, E. Cevik, A. Pivrikas, U. S. Schubert, D. A. Egbe, *Sol Energ Mat Sol C* **2010**, *94*, 484.
35. H. Wei, Y. H. Chao, C. Kang, C. Li, H. Lu, X. Gong, H. Dong, W. Hu, C. S. Hsu, Z. Bo, *Macromol Rapid Commun* **2015**, *36*, 84.

36. X. Gong, C. Li, Z. Lu, G. Li, Q. Mei, T. Fang, Z. Bo, *Macromol Rapid Commun* **2013**, *34*, 1163.
37. Y. Kan, Y. Zhu, Z. Liu, L. Zhang, J. Chen, Y. Cao, *Macromol Rapid Commun* **2015**.
38. S. H. Eom, S. Senthilarasu, P. Uthirakumar, S. C. Yoon, J. Lim, C. Lee, H. S. Lim, J. Lee, S.-H. Lee, *Org Electron* **2009**, *10*, 536.
39. S. Günes, H. Neugebauer, N. S. Sariciftci, *Chem. Rev.* **2007**, *107*, 1324.
40. A. S. Shalabi, S. Abdel Aal, M. M. Assem, *Nano Energy* **2012**, *1*, 608.
41. M. C. Scharber, D. Wuhlbacher, M. Koppe, P. Denk, C. Waldauf, A. J. Heeger, C. L. Brabec, *Adv. Mater.* **2006**, *18*, 789.
42. G. Malliaras, J. Salem, P. Brock, J. Scott, *J Appl Phys* **1998**, *84*, 1583.
43. P. W. M. Blom, V. D. Mihailetchi, L. J. A. Koster, D. E. Markov, *Adv. Mater.* **2007**, *19*, 1551.
44. C. J. Brabec, S. E. Shaheen, C. Winder, N. S. Sariciftci, P. Denk, *Appl Phys Lett* **2002**, *80*, 1288.

Chapter 4

Concluding Remarks

In this thesis, to fabricate and measure photoelectrical properties of polymer solar cell devices by using C60-PEG/PEDOT material and improving the Power conversion efficiency (PCE), the following research has been carried out: Preparation of C60- PEG/PEDOT composite material by using chemical oxidative polymerization under low temperature organic-solvents processed. Then fabrication of photovoltaic devices of polymer solar cells by using C60- PEG/PEDOT composite material and measurement their photoelectric properties. To improve the PCE, many methods had been implemented, in which biomimetic and other simple method were effective, including mimicking moth eye microstructure film and changing molar ratio of C60 and PEG.

1. The first, PEDOT was synthesized by using chemical oxidative polymerization. Then C60-PEG/PEDOT gel, which form interpenetrate network structure, was prepared under low temperature(<70℃) organic solvent processed.

2. The C60-PEG/PEDOT gel was coated onto ITO glass by using spin-coater under the condition of 1000-2500 rpm to form the porous C60-PEG/PEDOT film. Then the film using this material was identified by SEM, FT-IR, XRD, UV response and UV-Vis absorption spectra measurement. The results showed that PEDOT was synthesized inside of C60-PEG gel, and that the C60-PEG/PEDOT gel has an amorphous structure on contrary to C60-PEG crystalline structures. The bandgap of C60-PEG/PEDOT material is smaller than C60-PEG materials, that is, C60-PEG/PEDOT material is stronger absorption of UV light than C60-PEG material.

3. Then we fabricated the polymer solar cells device using this composite

material, and it was confirmed the composite film showed UV response and power conversion efficiency by irradiating with UV or simulated sunlight. The results showed that UV response of C60-PEG/PEDOT device was much higher than C60-PEG device. It was considered that UV response was improved by synthesizing PEDOT into C60-PEG gel to form new interpenetrate network structure.

4. PCE of C60-PEG/PEDOT device was about 1.2×10-3 %. Fabricated bulk heterojuction polymer solar cells device by using C60-PEG/PEDOT film, the Jsc is more 10 times higher than C60-PEG/Pc device. Improved the PCE by changing the molar ratio of C60 and PEG, the result showed the best PCE is $1.6x10^{-3}$, when molar ratio of C60 to PEG has been optimized to approximately 1:4.

5. Mimicking the unique antireflection functionalities of moth eye microstructure, microrods structure film with lots of nanoscale layered sheet on the rod were fabricated by template method at room temperature.

6. The top SEM images shown the microrods structure surface morphology, UV-Vis absorption spectra shown a significantly red shift of microrods structure film, it was estimated that it would be attributed to bandgap narrowing along with the structure changing. Then CV measurement provided a reference that the bandgap of microrods structure film was 0.08eV narrow than the flat structure film.

7. From the results of UV-Vis absorption and CV measurement, it was demonstrated that the microrods structure film would increase the light absorption.

8. Fabricated bulk heterojuction polymer solar cell devices by using

C60-PEG/PEDOT microrods material film, and measured the PCE, Which was more higher than the flat structure one

List of Publications

1. Zhang Huiqiu, Masaru Ichinose, Hideaki Takahashi, Shingo Tamesue, Tetsu Mitsumata, Masayuki Yagi, Norio Tsubokawa, Takeshi Yamauchi, "Preparation and Photoelectric Properties of C60-Poly(ethylene glycol) and Poly(3,4-ethylenedioxythiophene) Composite gel by low-temperature organic-solvents processed"
Polym. J. (accepted)

2.Huiqiu Zhang, Shingo Tamesue, Tetsu Mitsumata, Ryosuke Ishikawa, Nozomu Tsuboi, Masayuki Yagi, Norio Tsubokawa,Takeshi Yamauchi, "Preparation of Microrods Structure C60- PEG and PEDOT Composite Film by Template method and Application for Organic Photovoltaic Devices"
Macromol. Rapid Commun. (Submitted)

Acknowledgments

First of all, I would like to extend my sincere gratitude to Professor Dr. Takeshi Yamauchi at the Graduate School of Science and Technology, Niigata University, for his instructive advice and useful suggestions on my thesis. I am deeply grateful of his help in the completion of this thesis.

I would like to express my deeply gratitude to Professor Dr. Masayuki Yagi, Faculty of Engineering, Niigata University, who gives me the chance to become a doctor of Niigata University.

I would also like to express deeply thankful to Professor Dr. Takashi Kaneko, Niigata University for his reviewing this thesis.

I would like to express deeply indebted to Professor Norio Tsubokawa and Dr. Ryosuke Ishikawa of Niigata University, for their kind help with measurement of Power Conversion Efficiency of the devices.

I would also like to express deeply thankful to Associate Professor Tetsu Mitsumata, Assistant Professor Shingo Tamesue, Ms. Kumi Hashimoto and Mr. Hiroshi Saito of Niigata University for their kindly help on my research.

I am also deeply indebted to all current and former colleagues of Yamauchi laboratory for their direct and indirect help to me.

Special thanks should go to my friends for their care and assistance.

Finally, I wish to express his grateful thank to his parents, and his family, for their encouragement and support during this work.

Doctoral Program in Advanced Materials Science and Technology,
Graduate School of Science and Technology,
Niigata University,
July, 2015.